Title

Distinctive features of SARS-CoV-2-specific T cells predict recovery from severe COVID-19

Journal

Cell Reports, 36(3)

ISSN

2639-1856

Authors

Neidleman, Jason
Luo, Xiaoyu
George, Ashley F
et al.

Publication Date

2021-07-01

DOI

10.1016/j.celrep.2021.109414

Since January 2020 Elsevier has created a COVID-19 resource centre with free information in English and Mandarin on the novel coronavirus COVID-19. The COVID-19 resource centre is hosted on Elsevier Connect, the company's public news and information website.

Cell Reports

Article

Distinctive features of SARS-CoV-2-specific T cells predict recovery from severe COVID-19

Graphical abstract

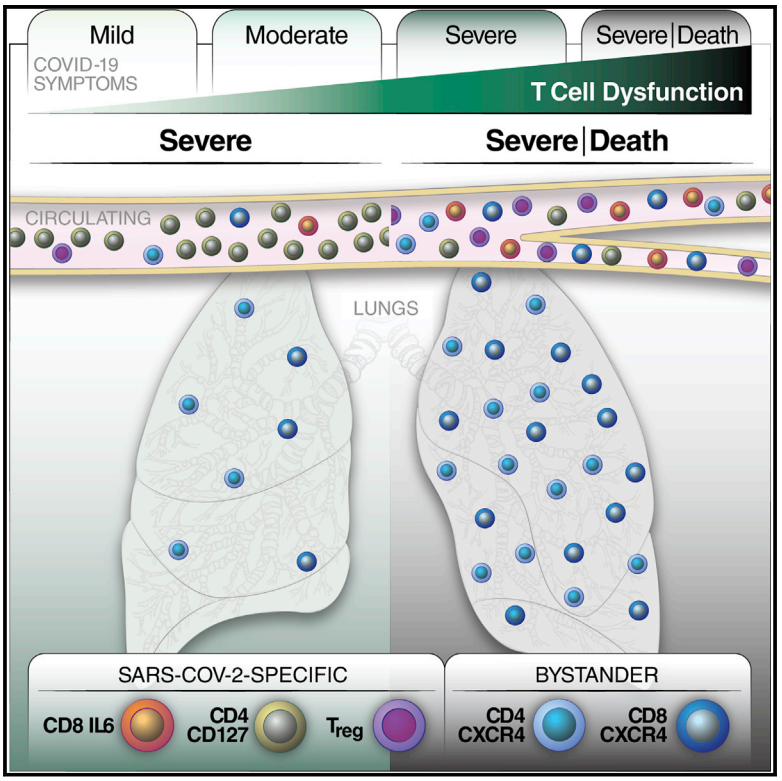

Authors

Jason Neidleman, Xiaoyu Luo, Ashley F. George, ..., Eliver Ghosn, Kara L. Lynch, Nadia R. Roan

Correspondence

eliver.ghosn@emory.edu (E.G.), kara.lynch@ucsf.edu (K.L.L.), nadia.roan@gladstone.ucsf.edu (N.R.R.)

In brief

Conducting CyTOF on cells from affected individuals, Neidleman et al. identify features of SARS-CoV-2-specific T cells predicting survival of severe COVID-19. Fatal COVID-19 is also characterized by escalating activation of bystander lung-homing CXCR4$^+$ T cells. Boosting SARS-CoV-2-specific T effector responses while diminishing CXCR4-mediated homing may help recovery from severe disease.

Highlights

- Dysfunctional spike-specific T cells are characteristic of severe COVID-19
- Spike-specific CD127$^+$ Th1 cells are increased in survivors of severe COVID-19
- Spike-specific Treg cells and IL6$^+$ CD8$^+$ T cells are increased in fatal COVID-19
- Escalation of activated lung-homing CXCR4$^+$ T cells is associated with fatal COVID-19

Neidleman et al., 2021, Cell Reports *36*, 109414
July 20, 2021
https://doi.org/10.1016/j.celrep.2021.109414

CellPress

Cell Reports

CellPress
OPEN ACCESS

Article

Distinctive features of SARS-CoV-2-specific T cells predict recovery from severe COVID-19

Jason Neidleman,[1,2,7] Xiaoyu Luo,[1,7] Ashley F. George,[1,2,7] Matthew McGregor,[1,2,7] Junkai Yang,[3] Cassandra Yun,[4] Victoria Murray,[5] Gurjot Gill,[5] Warner C. Greene,[1,6] Joshua Vasquez,[6] Sulggi A. Lee,[5] Eliver Ghosn,[3,*] Kara L. Lynch,[4,*] and Nadia R. Roan[1,2,8,*]

[1]Gladstone Institutes, San Francisco, CA 94158, USA
[2]Department of Urology, University of California, San Francisco, CA 94158, USA
[3]Deptartments of Medicine and Pediatrics, Lowance Center for Human Immunology, Emory Vaccine Center, Emory University, Atlanta, GA 30322, USA
[4]Department of Laboratory Medicine, University of California, San Francisco, CA 94110, USA
[5]Zuckerberg San Francisco General Hospital and the University of California, San Francisco, CA 94110, USA
[6]Department of Medicine, University of California, San Francisco, CA 94110, USA
[7]These authors contributed equally
[8]Lead contact
*Correspondence: eliver.ghosn@emory.edu (E.G.), kara.lynch@ucsf.edu (K.L.L.), nadia.roan@gladstone.ucsf.edu (N.R.R.)
https://doi.org/10.1016/j.celrep.2021.109414

SUMMARY

Although T cells are likely players in severe acute respiratory syndrome coronavirus 2 (SARS-CoV-2) immunity, little is known about the phenotypic features of SARS-CoV-2-specific T cells associated with recovery from severe coronavirus disease 2019 (COVID-19). We analyze T cells from 34 individuals with COVID-19 with severity ranging from mild (outpatient) to critical, culminating in death. Relative to individuals who succumbed, individuals who recovered from severe COVID-19 harbor elevated and increasing numbers of SARS-CoV-2-specific T cells capable of homeostatic proliferation. In contrast, fatal COVID-19 cases display elevated numbers of SARS-CoV-2-specific regulatory T cells and a time-dependent escalation in activated bystander CXCR4$^+$ T cells, as assessed by longitudinal sampling. Together with the demonstration of increased proportions of inflammatory CXCR4$^+$ T cells in the lungs of individuals with severe COVID-19, these results support a model where lung-homing T cells activated through bystander effects contribute to immunopathology, whereas a robust, non-suppressive SARS-CoV-2-specific T cell response limits pathogenesis and promotes recovery from severe COVID-19.

INTRODUCTION

The coronavirus disease 2019 (COVID-19) pandemic caused by severe acute respiratory syndrome coronavirus 2 (SARS-CoV-2) has taken an unprecedented toll on the world's healthcare systems and economy, and, a year after its emergence, had already claimed over 2 million lives, with fatality rates reaching as high as 20% in some countries (Sorci et al., 2020). Although most infected individuals are asymptomatic or mildly symptomatic, up to ~20% require hospitalization, and this rate increases dramatically in the elderly (>65 years) and those with underlying health conditions (Docherty et al., 2020; Grasselli et al., 2020). Evidence to date suggests variability in host response, rather than viral genetics, to be the prime driver behind the wide range of disease manifestations. For example, individuals genetically pre-disposed to low type I interferon (IFN) activity, because of inborn loss-of-function genetic variants or autoantibodies against these innate immune cytokines, have an increased risk of severe disease (Bastard et al., 2020; van der Made et al., 2020; Zhang et al., 2020).

The adaptive immune system, consisting of cellular (T cell) and humoral (B cell) immunity, is also important in host defense against SARS-CoV-2. Although a coordinated response between the cellular and humoral arms seems to be important in control (Rydyznski Moderbacher et al., 2020), T cells appear to be able to resolve infection when B cell responses are insufficient (Soresina et al., 2020). Furthermore, anti-SARS-CoV-2 antibody levels correlate with disease severity (Garcia-Beltran et al., 2021; Liu et al., 2019; Woodruff et al., 2020), suggesting that high antibody levels may not always be effective. A consistent hallmark of severe COVID-19 is T cell lymphopenia (Chen et al., 2020a; Zhao et al., 2020a), which is unlikely to simply reflect T cell sequestration in infected lungs (Liao et al., 2020). Importantly, although overall T cell lymphopenia is observed, the frequencies of some T cell subsets are associated positively with disease severity. For example, activated T cells and regulatory T (Treg) cells have been reported to be elevated in severe cases (De Biasi et al., 2020; Mathew et al., 2020). It is, however, unclear whether these T cells are specific to SARS-CoV-2.

Indeed, although many studies have profiled total T cells across the entire spectrum of COVID-19 severity, few have analyzed the features of T cells recognizing SARS-CoV-2 epitopes. Because these antigen-specific cells are the ones that

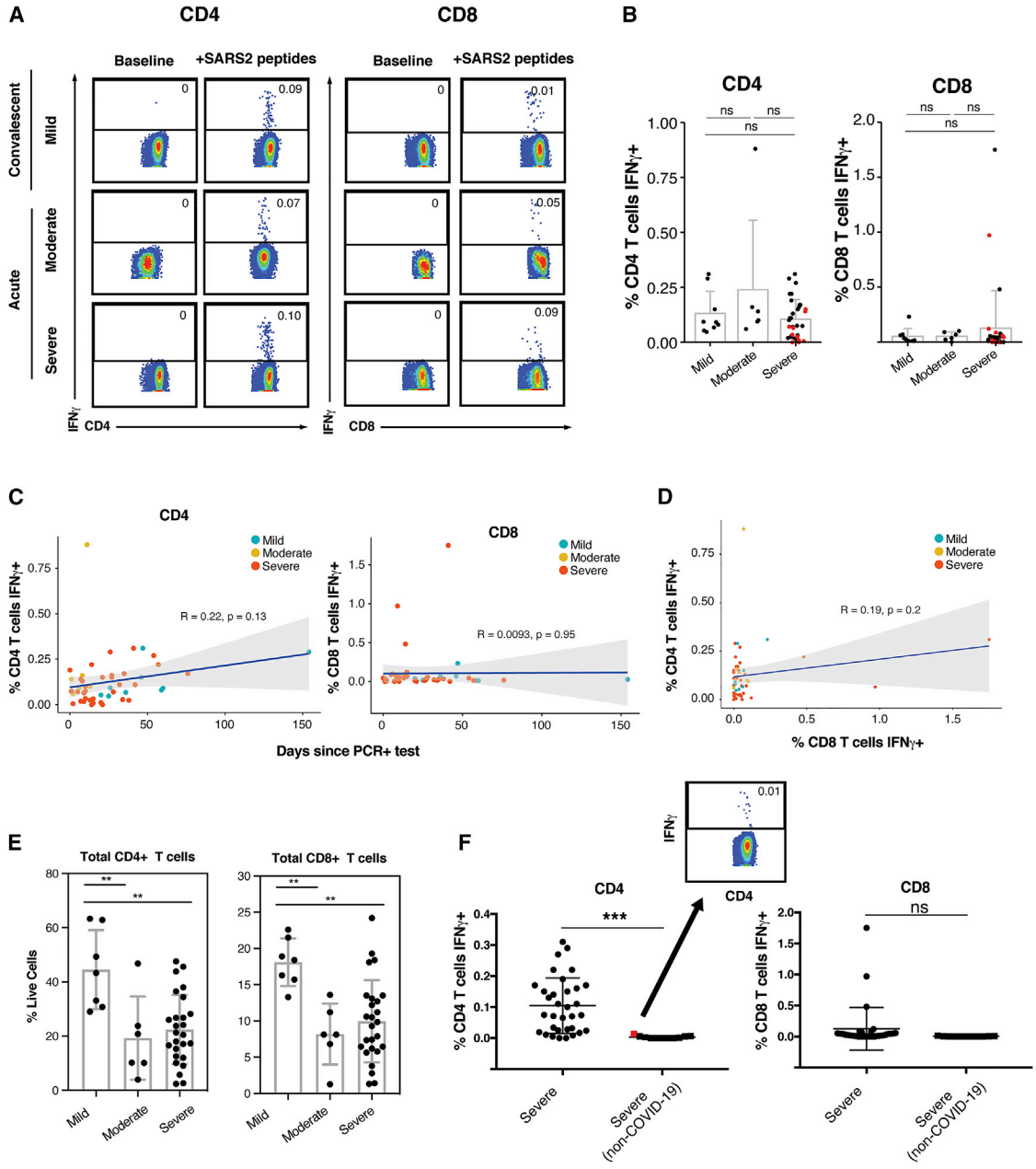

Figure 1. *De novo* IFNγ-producing SARS-CoV-2 spike-specific CD4$^+$ and CD8$^+$ T cells are elicited during mild, moderate, and severe COVID-19

(A) Pseudocolor plots of CyTOF datasets reflecting percentages of CD4$^+$ or CD8$^+$ T cells producing IFNγ at baseline or in response to 6-h stimulation with overlapping peptides from SARS-CoV-2 spike. Results are gated on live, singlet CD4$^+$ or CD8$^+$ T cells.

(B) Percentages of CD4$^+$ and CD8$^+$ T cells producing IFNγ in response to spike peptide stimulation in all COVID-19 cases. ns, non-significant as determined by one-way analysis of variance with a Bonferroni post-test. Datapoints in red correspond to individuals with severe disease who did not survive COVID-19 and will be discussed further in subsequent figures.

(C) The frequencies of SARS-CoV-2-specific T cells did not significantly correlate with time since initial SARS-CoV-2 PCR$^+$ test.

(D) The frequencies of SARS-CoV-2-specific CD4$^+$ and CD8$^+$ T cells did not significantly correlate with each other.

The scatterplots in (C) and (D) show the correlation coefficients (R) and p values, which were calculated using t distribution with n-2 degrees of freedom, and the 95% confidence intervals of the regression lines, which are shaded in gray.

(legend continued on next page)

can directly recognize virally infected cells and aid in generation of SARS-CoV-2-specific antibodies, they have the most potential to exert a beneficial effect on recovery from disease. We recently demonstrated that SARS-CoV-2-specific T cells from convalescent individuals who had recovered from mild disease produced IFNγ but not interleukin-4 (IL-4), IL-6, or IL-17 (Neidleman et al., 2020a). The undetected cytokines, particularly IL-6, have been implicated in COVID-19-associated pathogenesis (Del Valle et al., 2020; Hotez et al., 2020; Huang et al., 2020; Mathew et al., 2020; Pacha et al., 2020; Zhou et al., 2020a), although whether SARS-CoV-2-specific T cells secrete these cytokines during severe disease, and, if so, whether this contributes to pathogenesis, is not clear. In fact, the fundamental question of whether SARS-CoV-2-specific T cells are beneficial or detrimental during acute infection is debated. A recent study found that a robust SARS-CoV-2-specific T cell response, but not a strong antibody response, is negatively associated with disease severity (Rydyznski Moderbacher et al., 2020), whereas another research group reported a pathogenic role of SARS-CoV-2-specific T cells (Anft et al., 2020; Thieme et al., 2020). Differences in experimental design may account for these discrepant results, but, importantly, these prior studies did not compare fatal with non-fatal COVID-19 cases. Most studies to date have compared immune features associated with moderate versus severe COVID-19 cases, and to our knowledge, no studies have compared the phenotypes of SARS-CoV-2-specific T cells in individuals with severe COVID-19 who ultimately recover from or succumb to disease.

Here we define the features of T cells from individuals hospitalized in the ICU for COVID-19, including some that recovered and some that died from disease. We implemented deep phenotyping of total and SARS-CoV-2-specific T cells using 38-parameter CyTOF. By conducting longitudinal assessments of 34 individuals with COVID-19 with disease manifestations ranging from mild to fatal, we identified unique phenotypic features of SARS-CoV-2-specific and bystander T cells associated with recovery from severe disease and paired this analysis with a detailed examination of the features of T cells in the lungs of individuals with COVID-19.

RESULTS

Cohorts and experimental design

We analyzed a total of 48 blood specimens from 34 SARS-CoV-2-infected individuals, 33 of which were from individuals hospitalized in the ICU ("severe") and 6 from individuals hospitalized but not in the ICU ("moderate"). The last 9 came from individuals who were never hospitalized ("mild") (STAR Methods). An additional 11 SARS-CoV-2-negative individuals hospitalized in the ICU were phenotyped by CyTOF. Immediately following PBMC isolation, a portion of the cells was fixed for CyTOF, and the remaining cells were stimulated with overlapping peptides from SARS-CoV-2 spike to enable detection of induced cytokines. The unstimulated ("baseline") and peptide-stimulated specimens were analyzed simultaneously using the CyTOF panel presented in STAR Methods.

SARS-CoV-2-specific T cells are elicited during mild, moderate, and severe COVID-19

Manual gating was used to identify $CD4^+$ and $CD8^+$ T cells from the 59 specimens. Because activation markers, but not IFNγ, were expressed in the baseline specimens (Figure S1A; Figure 1A), we used IFNγ to identify SARS-CoV-2-specific T cells in the stimulated samples. Although cells producing high levels of IFNγ were readily identified following peptide stimulation (Figure 1A), cells producing high levels of the cytokines IL-4, IL-5, IL-6, or IL-17 were not observed (Figures S1B and S1C). Their frequencies ranged from undetectable to almost 2% of T cells, were not significantly different between the groups of individuals (Figure 1B), and did not correlate with time since initial PCR^+ test (Figure 1C). They were also not correlated between $CD4^+$ and $CD8^+$ T cells (Figure 1D). In comparison, total (non-antigen-specific) $CD4^+$ and $CD8^+$ T cell frequencies from the baseline specimens were diminished significantly in the moderate and severe groups (Figure 1E), consistent with the lymphopenia reported previously in hospitalized, acutely infected individuals (Chen et al., 2020a; Zhao et al., 2020a).

Because cross-reactive T cell responses have been reported in some individuals never exposed to SARS-CoV-2 (Braun et al., 2020; Grifoni et al., 2020; Sekine et al., 2020), we assessed to what extent the responses we detected in individuals with COVID-19 were generated *de novo*. We acquired 11 fresh blood specimens from individuals hospitalized in the ICU for reasons unrelated to COVID-19 and confirmed by RT-PCR to not be infected with SARS-CoV-2. SARS-CoV-2-specific $CD4^+$ T cells were significantly more frequent in infected than uninfected individuals in the ICU (Figure 1F). Although we saw evidence of low levels of cross-reactive responses, even in the uninfected individual with the strongest response to peptide stimulation, SARS-CoV-2-specific cells only accounted for 0.01% of CD4+ T cells (Figure 1F, inset). SARS-CoV-2-specific $CD8^+$ T cells recognizing spike were also detected at higher frequencies in infected relative to uninfected individuals, but this did not reach statistical significance (Figure 1F). These data suggest that, despite lymphopenia, *de novo* T cell responses are mounted against SARS-CoV-2 in individuals hospitalized for COVID-19.

Phenotypes of total and SARS-CoV-2-specific T cells differ in mild, moderate, and severe COVID-19

As an initial examination of the T cells in infected individuals, we calculated the mean signal intensity (MSI) of each antigen (Figure S2) and compared them between the 3 patient groups for

(E) Evidence of T cell lymphopenia in specimens from moderate and severe COVID-19 relative to mild cases. The frequencies of total $CD4^+$ and $CD8^+$ T cells were determined in the baseline (non-stimulated) specimens. $^{**}p < 0.01$ as determined by one-way analysis of variance with a Bonferroni post-test.
(F) Proportion of IFNγ-producing cells among T cells from individuals in the ICU with or without SARS-CoV-2 infection. Even in the uninfected specimen with the highest response to spike stimulation (red dot), the proportion of IFNγ-producing cells was only 0.01% (inset), suggesting that the responses we detected in COVID-19 specimens corresponded to *de novo* SARS-CoV-2-specific T cells. $^{***}p < 0.001$ as determined by a Student's unpaired t test.
Each datapoint corresponds to a different specimen (biological replicates). See also Figures S1 and S2.

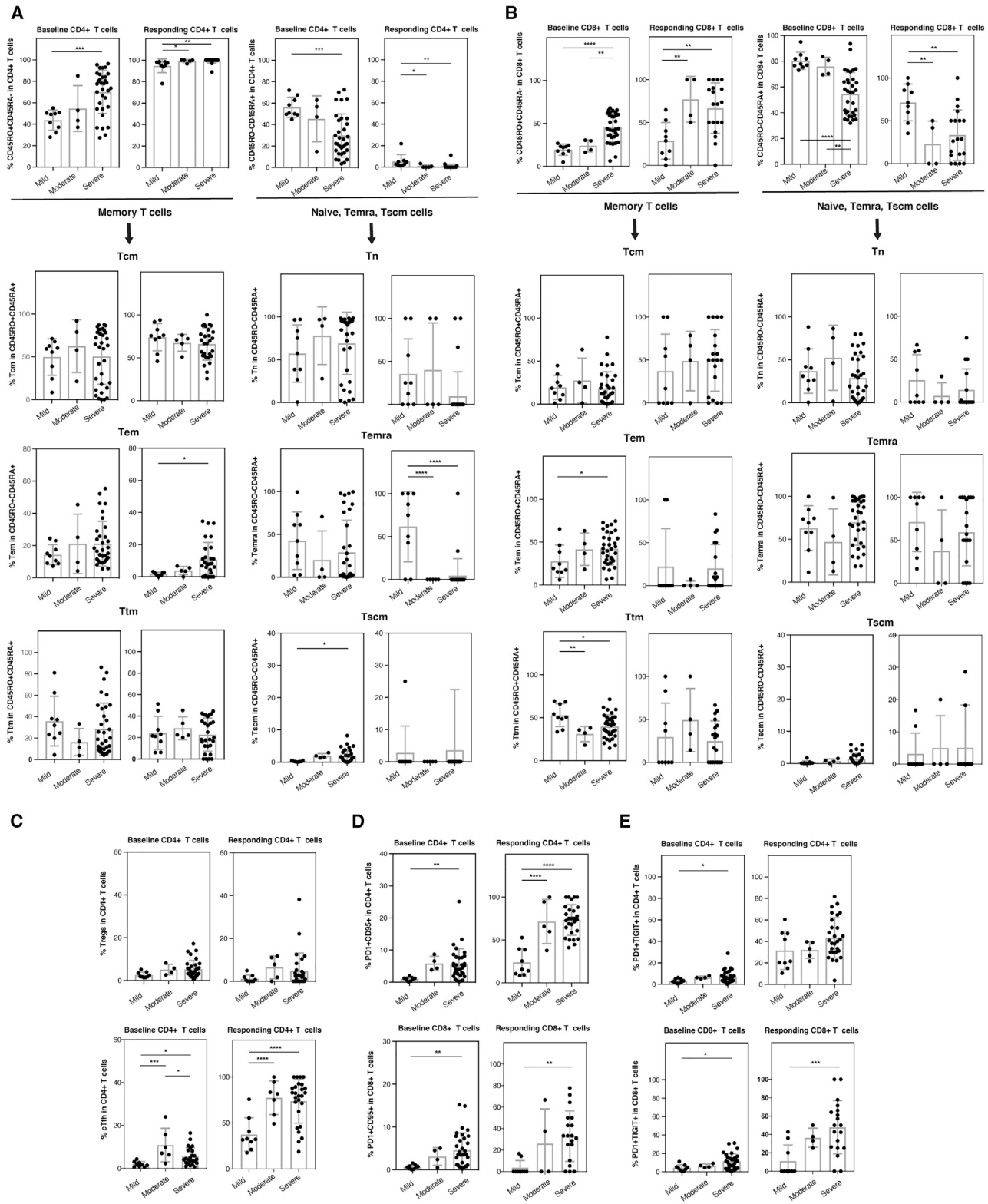

Figure 2. Subset distribution of total and SARS-CoV-2-specific T cells during mild, moderate, and severe COVID-19 by manual gating

(A and B) Distribution of baseline and SARS-CoV-2-specific $CD4^+$ (A) and $CD8^+$ (B) T cells from individuals with COVID-19 among memory ($CD45RO^+CD45RA^-$) and a mixture of Tn, Temra, and Tscm ($CD45RO^-CD45RA^+$) cells. Breakdown into further subsets was achieved by manually gating on subset marker

(legend continued on next page)

the following cell populations: baseline, bystander, and SARS-CoV-2 specific. Among baseline samples, $CD4^+$ and $CD8^+$ T cells from severe cases expressed significantly higher levels of the activation markers HLADR, CD69, CD25, and PD1 as well as the chemokine receptor CXCR4, which directs cells to inflamed and damaged lung tissues (Mamazhakypov et al., 2021), relative to mild cases. Among SARS-CoV-2-specific T cells, antigens significantly upregulated in severe relative to mild cases included the activation/exhaustion markers PD1 and TIGIT.

We next assessed the subset distribution of total and SARS-CoV-2-specific T cells by manual gating. CD45RO expression is commonly used to define memory T cells and CD45RA to define naive (Tn) cells, although CD45RA is also expressed on terminally differentiated effector memory T (Temra) cells and stem cell memory T (Tscm) cells. We found that, for $CD4^+$ and $CD8^+$ T cells, $CD45RO^+CD45RA^-$ frequencies were highest in the severe group, and $CD45RO^-CD45RA^+$ were the lowest (Figures 2A and 2B). This was observed for total and SARS-CoV-2-specific T cells. Gating within the $CD45RO^+CD45RA^-$ and $CD45RO^-CD45RA^+$ populations allowed us to identify the proportions of central memory T (Tcm), effector memory T (Tem), transitional memory T (Ttm), Tn, Temra, and Tscm subsets (Figures 2A and 2B). SARS-CoV-2-specific $CD4^+$ T cells were enriched for Tem cells and relatively depleted of Temra cells. Changes in subset distribution were also observed among total T cells. For example, the severe group harbored significantly higher proportions of $CD8^+$ Tem and $CD4^+$ Tscm cells and lower proportions of $CD8^+$ Ttm cells.

We then examined the percentages of $CD4^+$ Treg cells and circulating T follicular helper (cTfh) cells, subsets important in immunoregulation and helping antibody responses, respectively. The frequencies of Treg cells were similar between the three groups of individuals, although there was a trend for higher levels in the severe group. In contrast, the moderate and severe groups had significantly higher frequencies of SARS-CoV-2-specific cTfh than the mild group (Figure 2C), suggesting potential elicitation of antibody production through T cell help during moderate/severe acute infection. Additional manual gating revealed $PD1^+CD95^+$ T cells within the total and SARS-CoV-2-specific compartments to be most abundant during severe infection (Figure 2D). Total and SARS-CoV-2-specific $PD1^+TIGIT^+$ T cells were also more frequent during severe infection, but only within the CD8 compartment (Figure 2E). These findings are consistent with the increased expression of PD1, CD95, and TIGIT in severe cases (Figure S2). Because co-expression of PD1 and CD95 is characteristic of apoptosis-prone cells, whereas co-expression of PD1 and TIGIT is characteristic of exhausted cells, these findings together suggest increased T cell dysfunction during severe COVID-19.

Clustering reveals an accumulation of activation and exhaustion markers in T cells from individuals with severe COVID-19

Having analyzed cellular subsets through manual gating, we then implemented a more holistic approach by integrating all phenotyping markers in our panel to identify populations of cells associated with disease severity. Clustering by FlowSOM (Van Gassen et al., 2015) revealed differences between mild, moderate, and severe infection in total and SARS-CoV-2-specific T cells and among the $CD4^+$ (Figures 3A–3D) and $CD8^+$ (Figures 4A–4D) compartments. Among total $CD4^+$ T cells, the most noticeable difference was a single cluster (B4.9), composed of activated memory $CD4^+$ T cells expressing high levels of the lung-homing receptor CCR6 (Ito et al., 2011), that was present at higher frequency in the severe group (Figure 3E). Analysis of total $CD8^+$ T cells revealed four clusters that were significantly enriched in the severe group (Figure 4E). These clusters expressed elevated levels of HLADR, but only some expressed CD38 (Figure 4F), suggesting that HLADR may be a more universal marker of SARS-CoV-2-induced global T cell activation than CD38. One cluster (B8.1) was enriched in the mild group (Figure 4E), albeit insignificantly, and this cluster expressed low levels of HLADR and CD38 (Figure 4F).

Examination of SARS-CoV-2-specific T cell clusters revealed one $CD4^+$ and one $CD8^+$ T cell cluster enriched in the severe group and one $CD4^+$ T cell cluster enriched in the mild group (Figures 3G and 4G). The two clusters enriched in the severe group shared phenotypic features, including increased expression levels of the activation markers HLADR and CD38 and exhaustion markers PD1 and CTLA4 and decreased expression of the IL-7 receptor alpha chain CD127 (Figures 3H and 4H). These markers were not differentially expressed among the $CD4^+$ cluster enriched in the mild group (Figure 3H). To determine whether a subset of the markers identified by FlowSOM is sufficient to enrich for cells from the severe group, we manually gated on cells expressing the two activation/exhaustion markers PD1 and CTLA4. $PD1^+CTLA4^+$ cells were more frequent in the severe groups among SARS-CoV-2-specific $CD4^+$ and $CD8^+$ T cells (Figures 3I and 4I). These findings point to an overabundance of exhausted T cells recognizing SARS-CoV-2 spike during severe COVID-19, consistent with increased severity-associated T cell dysfunction.

Recovery from severe COVID-19 is associated with enhanced SARS-CoV-2-specific effector T cell response

Of our specimens analyzed by CyTOF, 33 were from SARS-CoV-2-infected individuals in the ICU, 32% of whom subsequently died from COVID-19. We next focused on these specimens to try to

combinations. Downstream of the CD45RO and CD45RA gates, we defined the subsets as follows: Tcm ($CD27^+CCR7^+$), Tem ($CD27^-CCR7^-$), Ttm ($CD27^+CCR7^-$), Tn ($CCR7^+CD95^-$), Temra ($CCR7^-$), Tscm ($CCR7^+CD95^+$).

(C) Proportions of Treg ($CD45RO^+CD45RA^-CD25^+CD127^{low}$) and cTfh ($PD1^+CXCR5^+$) cells among baseline and SARS-CoV-2-specific $CD4^+$ T cells from individuals with COVID-19.

(D) The proportion of apoptosis-prone ($PD1^+CD95^+$) cells among $CD4^+$ and $CD8^+$ T cells is increased in severe COVID-19 cases for total and SARS-CoV-2-specific T cells.

(E) The proportion of exhausted cells ($PD1^+TIGIT^+$) among total and SARS-CoV-2-specific $CD8^+$ T is increased in severe COVID-19. *$p < 0.05$, **$p < 0.01$, ***$p < 0.001$, ****$p < 0.0001$, as determined by one-way analysis of variance with a Bonferroni post-test.

Each datapoint corresponds to a different specimen (biological replicates).

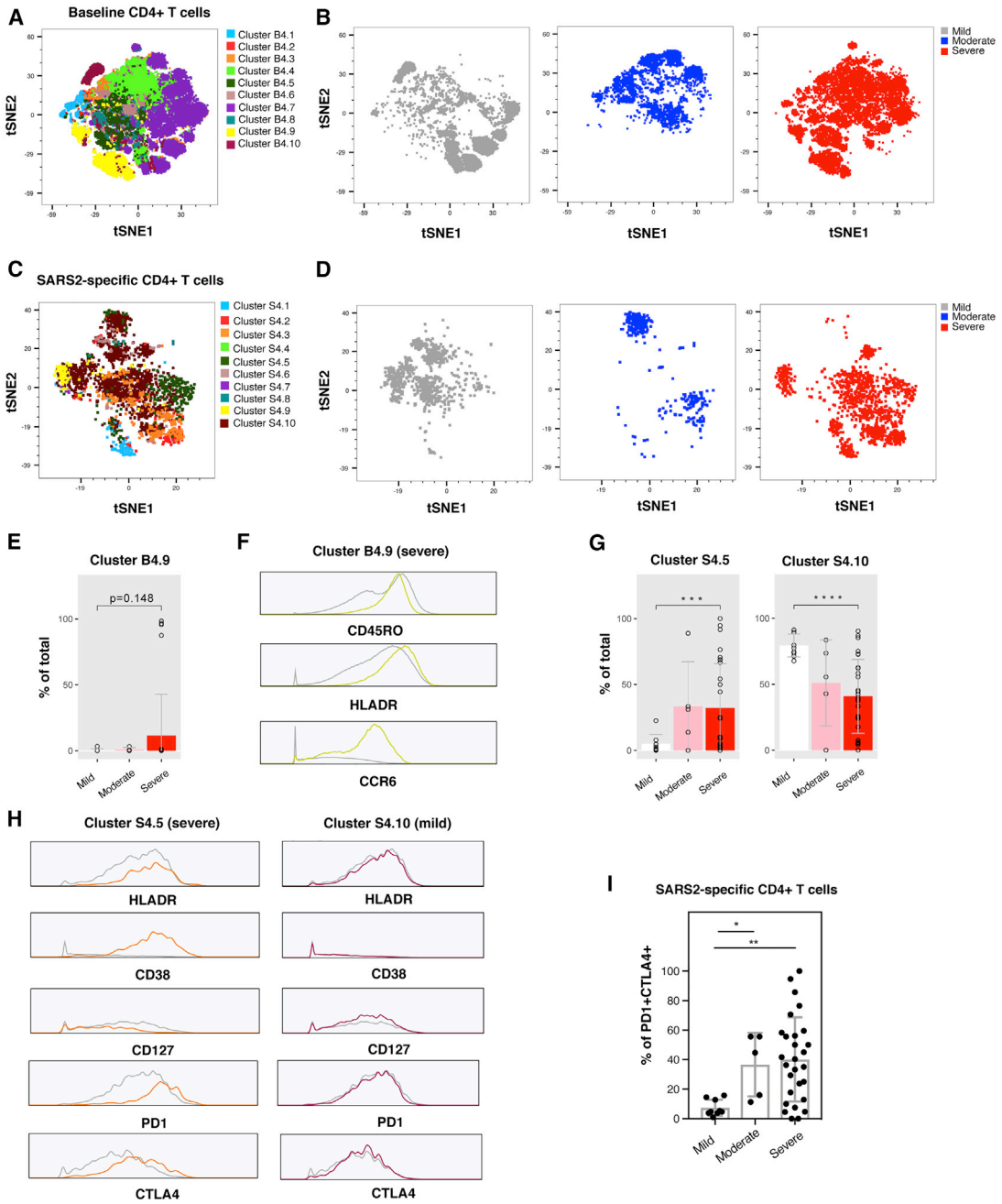

Figure 3. Clustering reveals enrichment in activated and exhausted SARS-CoV-2-specific CD4⁺ T cells during severe COVID-19

(A and C) FlowSOM clustering of total (baseline, A) and SARS-CoV-2-specific (C) CD4⁺ T cells from all infected groups, visualized as a t-SNE plot. Ten clusters were identified. Each cluster name begins with "B" (for baseline) or "S" (for SARS-CoV-2-specific), followed by "4" (for CD4).

(B and D) Total (B) and SARS-CoV-2-specific (D) CD4⁺ T cells from mild (gray), moderate (blue), and severe (red) COVID-19 map to different areas of the t-SNE, indicating that they have different phenotypes.

(A) and (B) share the same t-SNE space, and (C) and (D) share the same t-SNE space.

(E) Proportion of total CD4⁺ T cells in the B4.9 cluster in the three groups.

(F) High expression levels of the memory marker CD45RO, activation marker HLADR, and chemokine receptor CCR6 in cells from the B4.9 cluster (yellow trace) relative to total CD4⁺ T cells (gray trace).

(G) Proportion of SARS-CoV-2-specific CD4⁺ T cells in the S4.5 and S4.10 clusters across the three groups. ***$p < 0.001$ and ****$p < 0.0001$ as determined by Student's unpaired t test and adjusted for multiple testing using Bonferroni for false discovery rate (FDR).

(legend continued on next page)

identify T cell signatures associated with survival of severe disease. Age did not account for the differential survival outcomes because the ages of survivors and non-survivors were not significantly different. Although male sex is a risk factor for severe COVID-19, we found, among our individuals in the ICU, a lower proportion of males who died (22% compared with 40% for females). Furthermore, we found similar frequencies of SARS-CoV-2-specific T cells among our hospitalized male and female individuals and no marked phenotypic differences, although there was a trend of higher activation of SARS-CoV-2-specific T cells in females (Figure S3), consistent with previous reports of total HLADR$^+$CD38$^+$ T cells being higher in female individuals with COVID-19 (Takahashi et al., 2020). Because prior studies found high levels of SARS-CoV-2 antibodies to be associated with more severe disease (Garcia-Beltran et al., 2021; Liu et al., 2019; Woodruff et al., 2020), we assessed whether immunoglobulin G (IgG) and IgM against the SARS-CoV-2 spike and nucleocapsid were enriched in non-survivors. We did not find this to be the case, although we observed moderate/severe cases to harbor higher levels of antibodies than mild cases (Figure S3).

We then examined whether T cells from survivors and non-survivors differed in their response to spike peptide stimulation. Non-survivors more frequently failed to mount a robust SARS-CoV-2-specific T cell response, particularly for CD4$^+$ T cells (Figure 5A). The SARS-CoV-2-specific CD8$^+$ T cell response trended higher in survivors, but this did not reach statistical significance because of lower overall responses. Individuals who mounted detectable SARS-CoV-2-specific T cell responses harbored significantly lower frequencies of total HLADR$^+$CD69$^+$ CD4$^+$ and CD8$^+$ T cells (Figure S4), suggesting that an overall heightened state of T cell activation may hinder development of T responses directed specifically against SARS-CoV-2.

Interestingly, two individuals mounted very robust CD8$^+$ T cell responses to spike peptides, and one of these survived whereas the other did not (highlighted in blue and red, respectively, in Figure 5A). After comparing all antigens on these two individuals' CD8$^+$ T cells, we found that IL-6 levels within SARS-CoV-2-specific CD8$^+$ T cells were lower in the survivor than in the non-survivor, and this phenomenon was not observed among total CD8$^+$ T cells (Figure 5B). The subtleness of the increase in IL-6 in SARS-CoV-2-specific CD8$^+$ T cells from the non-survivor was not due to poor antibody quality because a positive control of LPS-stimulated monocytes led to robust detection of IL-6 (Figure 5C). This observation prompted us to examine IL-6 expression among all ICU individuals that did elicit SARS-CoV-2-specific CD8$^+$ T cell responses. Indeed, we found a highly significant increase in IL-6-producing, SARS-CoV-2-specific CD8$^+$ T cells in non-survivors but not among total CD8$^+$ T cells (Figure 5B). These results suggest the possibility that SARS-CoV-2-specific CD8$^+$ T cells producing IFNγ and IL-6 may contribute to lethal immunopathogenesis, although follow-up studies will be needed to confirm this hypothesis.

We next assessed whether the major T cell subsets were differentially distributed among survivors and non-survivors. Memory CD4$^+$ T cells were statistically more frequent in survivors, but no significant differences were observed among the Tcm, Tem, Ttm, Tn, Temra, or Tscm subsets (Figure S5). Interestingly, however, SARS-CoV-2-specific Treg cells were significantly more frequent among non-survivors but total Treg cells were not (Figure 5D). In contrast, Tfh cell frequencies were equivalent between survivors and non-survivors (Figure 5D). These observations are consistent with a model where Treg cells recognizing SARS-CoV-2 spike can hinder elicitation of a robust SARS-CoV-2-specific T cell response and prevent recovery from severe disease.

Clustering reveals more activated, long-lived SARS-CoV-2-specific CD4$^+$ T cells in survivors of severe COVID-19

To compare T cells from survivors and non-survivors in an unbiased fashion, we subjected them to clustering via FlowSOM and found phenotypic differences between the two groups for CD4$^+$ (Figures 6A and 6B) and CD8$^+$ (Figures S6A and S6B) T cells. Among total CD4$^+$ T cells, two clusters (B4.1 and B4.9) were enriched in the survivor group, although the former did not meet statistical significance (Figure 6C). Both clusters consisted of activated (HLADR$^+$) memory (CD45RO$^+$) cells. Although B4.1 expressed the additional activation markers CD38, CD69, and CCR5, B4.9 did not, consistent with earlier observations of HLADR being a more universal marker of T cell activation. Similar analyses among total CD8$^+$ T cells revealed cluster B8.6 to be more frequent among survivors, albeit insignificantly, after multiple correction (Figure S6C). This cluster also harbored activated cells, and these were predominantly Tem cells, as suggested by low expression of CCR7 and CD62L. Interestingly, of all CD8$^+$ T cell clusters, this one harbored the highest levels of HLADR (Figure S6D). These results support the concept that global CD4$^+$ and CD8$^+$ T cell activation, as assessed by canonical activation markers such as HLADR, is not detrimental but, at least in our cohort, associated with survival of severe COVID-19. This was further supported by our observation that activated CD4$^+$ and CD8$^+$ T cells identified by manual gating were significantly higher in the survivor than the non-survivor groups (Figures 6D and S6E).

We then assessed the SARS-CoV-2-specific T cells. Among the CD4$^+$ T cells, S4.5 was increased in non-survivors, whereas S4.9 was increased in the survivors. Although S4.5 exhibited features of exhausted T cells (expressing high levels of PD1 and CTLA4), S4.9 exhibited features of cTfh cells with high proliferative potential (expressing high levels of CXCR5 and CD127) (Figure 6E). Manual gating confirmed a significant increase in CD127-expressing SARS-CoV-2-specific CD4$^+$ T cells in individuals who survived severe disease (Figure 6F). Because cluster S4.9 also expressed high levels of the activation marker CD69

(H) Cluster S4.5 cells express elevated levels of the activation markers HLADR and CD38 and the exhaustion markers PD1 and CTLA4 but diminished levels of the IL-7 receptor alpha chain CD127 (orange traces) relative to all SARS-CoV-2-specific CD4$^+$ T cells (gray traces); cluster S4.10 cells (maroon traces) do not.
(I) Increased frequencies of exhausted (PD1$^+$CTLA4$^+$) cells among SARS-CoV-2-specific CD4$^+$ T cells in severe COVID-19 samples, as validated by manual gating. *$p < 0.05$ and **$p < 0.01$ as determined by one-way analysis of variance with a Bonferroni post-test.
Datapoints from graphs with significance tests correspond to individual specimens (biological replicates).

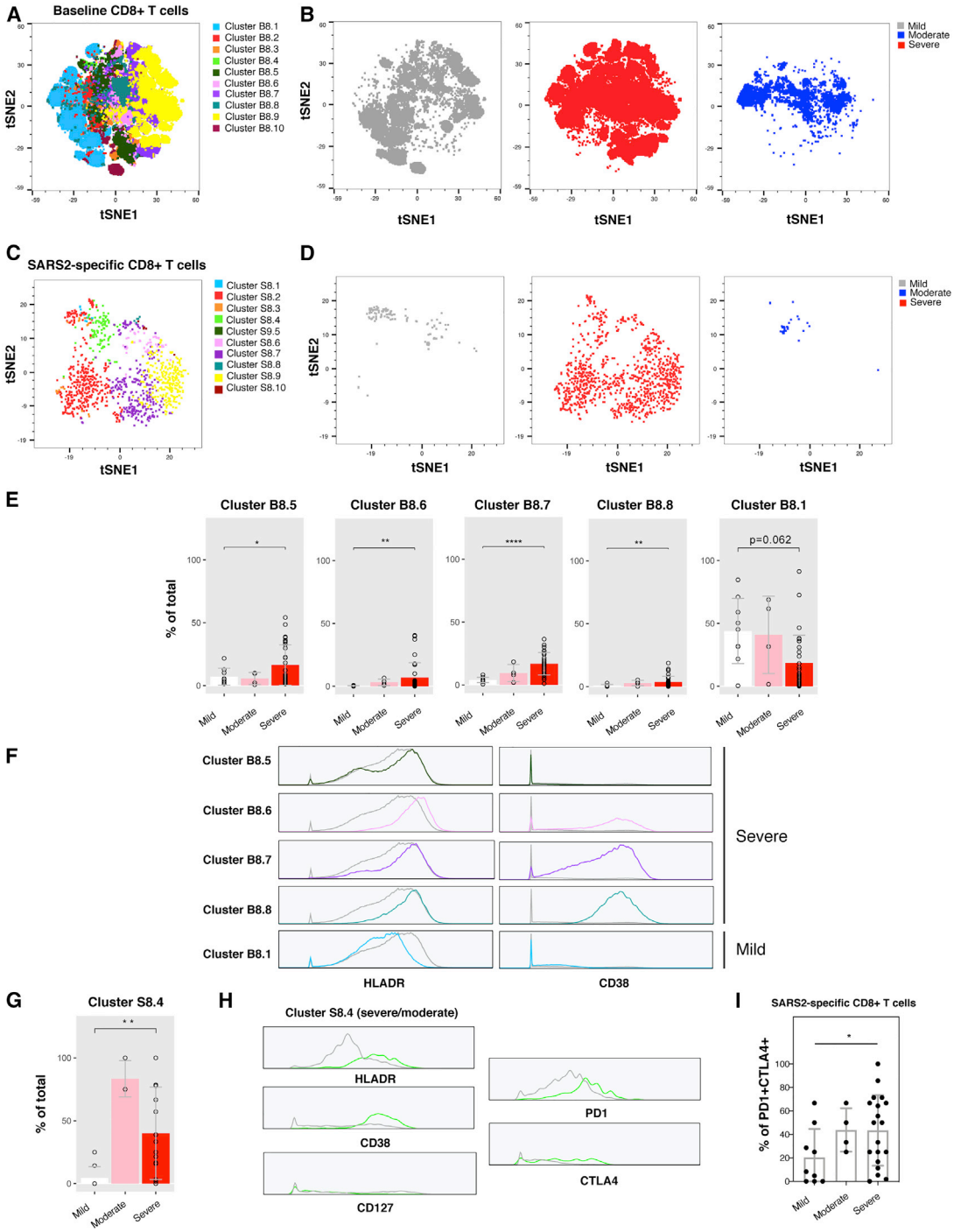

Figure 4. Clustering reveals enrichment of activated, exhausted SARS-CoV-2-specific CD8$^+$ T cells during severe COVID-19

(A and C) FlowSOM clustering of total (baseline, A) and SARS-CoV-2-specific (C) CD8$^+$ T cells from all infected groups, visualized as t-SNE plots. Ten clusters were identified. Each cluster name begins with "B" (for baseline) or "S" (for SARS-CoV-2-specific), followed by "8" (for CD8).

(B and D) Total (B) and SARS-CoV-2-specific (D) CD8$^+$ T cells from mild (gray), moderate (blue), and severe (red) COVID-19 map to different areas of the t-SNE, indicating that they have different phenotypes.

(E) Clusters B8.5, B8.6, B8.7, and B8.8 of total CD8$^+$ T cells are significantly enriched in the severe group, whereas there is a trend for cluster B8.1 enrichment in the mild group. *$p < 0.05$, **$p < 0.01$, and ****$p < 0.0001$ as determined by Student's unpaired t test and adjusted for multiple testing using Bonferroni for FDR.

(F) Cells from the B8.5, B8.6, B8.7, and B8.8 (severe-enriched) clusters express high levels of the activation marker HLADR (colored traces) relative to total CD8$^+$ T cells (gray trace), whereas the activation marker CD38 is elevated in only a subset of these clusters (colored traces) relative to total CD8$^+$ T cells (gray trace). Cells from the B8.1 (mild-enriched) cluster express low levels of both activation markers.

(legend continued on next page)

(Figure 6E), we assessed whether activated CD127$^+$ cells were increased in survivors and found this to be the case (Figure 6G). Further analysis of cluster S4.9 confirmed it to be highly activated (expressing the activation markers HLADR, CD38, CCR5, and Ox40 in addition to CD69), exhibit features of Tcm cells (expressing high levels of CCR7 and CD62L), and have mucosal tissue-homing potential (expressing high levels of CCR6 and CD49d) (Figure S7). In contrast, cluster S4.5 did not harbor most of these features (Figure S7). A cluster of SARS-CoV-2-specific CD8$^+$ T cells significantly enriched in survivors was also identified (S8.2), and this cluster harbored phenotypic features distinct from the cluster of survivor-associated SARS-CoV-2-specific CD4$^+$ T cells (Figure S6F). S8.2 was not activated (expressing low levels of HLADR and CD38) and, unlike S4.9, expressed low levels of CD127. Accordingly, unlike what was observed among SARS-CoV-2-specific CD4$^+$ T cells, the percentages of CD127-expressing cells among SARS-CoV-2-specific CD8$^+$ T cells were not increased among survivors (Figure S6G). This suggests that, relative to their CD4$^+$ counterparts, SARS-CoV-2-specific CD8$^+$ T cells in survivors may be less long-lived, although the observation that these cells express low levels of the terminal differentiation marker CD57 (Figure S6F) suggests that they may be able to differentiate through non-homeostatic proliferative mechanisms.

Escalating levels of SARS-CoV-2-specific T cells and dampening of bystander lung-homing activated cells predicts recovery from severe COVID-19

Finally, to better understand T cell features associated with survival of severe COVID-19, we assessed longitudinal specimens from our ICU cohort (STAR Methods). Although survivors tended to increase the frequency of SARS-CoV-2-specific T cells over time, non-survivors tended to not have much of these cells to begin with, or the frequency of these cells stagnated or decreased over time (Figures 7A and 7B). We then analyzed the high-dimensional phenotyping datasets of the longitudinal specimens for predictors of survival. Interestingly, total CD4$^+$ and CD8$^+$ T cells co-expressing CD69 and CXCR4 decreased over time in survivors, whereas the opposite was observed for non-survivors. Correspondingly, CD69$^-$CXCR4$^-$ T cell frequencies increased in the days leading up to discharge from hospital, whereas they decreased in the days leading up to death (Figure 7C). Because CD69 is an activation marker, and CXCR4 directs cells to various tissues, including inflamed and damaged lungs (Mamazhakypov et al., 2021), these observations support a model where activated bystander T cells recruited to the lungs lead to poor disease outcome.

To provide further support for this model, we mined a public single-cell RNA sequencing (scRNA-seq) dataset (Liao et al., 2020) of bronchoalveolar lavage (BAL) specimens from individuals with severe/critical COVID-19 and compared it with BAL fluid from individuals with moderate COVID-19 who harbored lower lung viral loads (Figure 7D). Elevated expression of CXCR4 was observed in T but not epithelial cells of individuals with severe disease (Figure 7E). Visualization of the T cells by UMAP (Figures 7F and S8A) revealed co-expression of CXCR4 and CD69 in the same subsets (Figure 7G). These cells likely infiltrated from the periphery because they express low levels of the T resident memory (Trm) marker CD103 (Figure 7H). To assess whether pulmonary T cells may themselves recruit more CXCR4$^+$ T cells, we assessed for expression of the CXCR4 ligands CXCL12 and HMGB1 (Schiraldi et al., 2012). Although CXCL12 was not detected (Figure S8B), HMGB1 was, particularly in a subset of CD8$^+$ T cells over-represented in individuals with severe disease (Figure 7I). These CD8$^+$ T cells comprise a unique cluster (Figure S8C) and express relatively low levels of CXCR4 but high levels of CD103, suggesting that they are mostly Trm cells. These data suggest that, during severe COVID-19, activated bystander T cells may, through expression of CXCR4, be recruited to the lung by HMGB1 produced by pulmonary cells, particularly CD8$^+$ Trm cells, which could contribute to COVID-19-associated mortality.

DISCUSSION

T cell lymphopenia was identified early during the COVID-19 pandemic as a hallmark of severe disease, implying an important role of T cells in control of SARS-CoV-2. However, the T cell subsets that may contribute to recovery and the role of T cells directly recognizing SARS-CoV-2 epitopes have not been investigated in depth. In this study, we compared total and SARS-CoV-2-specific T cells from individuals with mild, moderate, and severe COVID-19 and, within the severe cases, conducted in-depth analyses of longitudinal specimens to identify features predicting who will survive severe COVID-19. As discussed below, we discovered T cell features associated with recovery from disease but also some implicated in disease pathogenesis. As part of our study, we provide as a resource the raw CyTOF single-cell datasets for all total and SARS-CoV-2-specific T cells (STAR Methods).

Elevated levels of activated and exhausted T cells during severe COVID-19

The phenotypes of total T cells from individuals with COVID-19 from our study are largely consistent with a recent study that conducted deep profiling of immune cells (including T cells) using high-parameter flow cytometry (Mathew et al., 2020). We, like the prior study, had observed higher frequencies of CD8$^+$ Ttm cells in individuals with mild disease and a higher frequency of activated, PD1-expressing T cells in those with severe

(G) Cluster S8.4 is enriched in the severe and moderate groups relative to the mild group. **$p < 0.01$ as determined by Student's unpaired t test and adjusted for multiple testing using Bonferroni for FDR.
(H) Cluster S8.4 cells express elevated levels of the activation markers HLADR and CD38 and the exhaustion markers PD1 and CTLA4 but diminished levels of the IL-7 receptor alpha chain CD127 (green traces) relative to all SARS-CoV-2-specific CD8$^+$ T cells (gray traces).
(I) Increased frequencies of exhausted (PD1$^+$CTLA4$^+$) cells among SARS-CoV-2-specific CD8$^+$ T cells in severe relative to mild COVID-19, validated by manual gating. *$p < 0.05$ as determined by one-way analysis of variance with a Bonferroni post-test.
Datapoints from graphs with significance tests correspond to individual specimens (biological replicates).

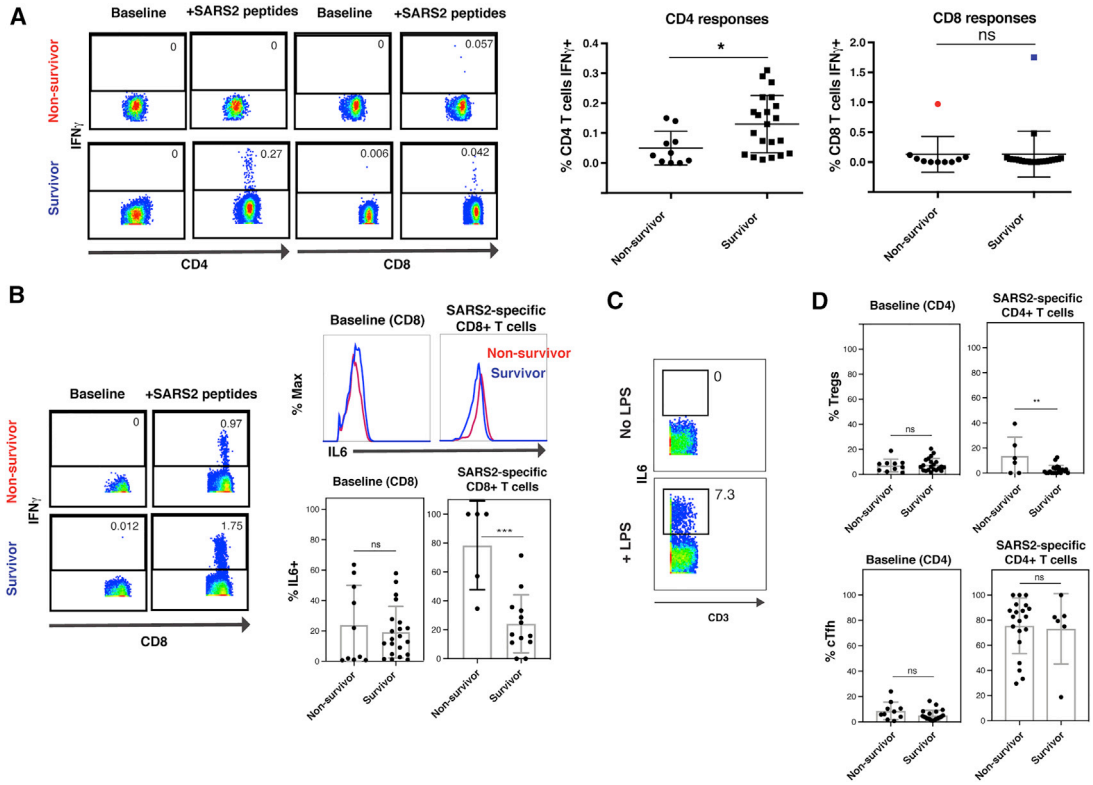

Figure 5. Distinct features of SARS-CoV-2-specific T cells are associated with recovery from severe COVID-19

(A) Higher frequencies of SARS-CoV-2-specific T cells in individuals with severe COVID-19 who survived ("survivor") than in those who did not ("non-survivor"). Left: pseudocolor plots reflecting the percentages of SARS-CoV-2-specific T cells from representative infected individuals in the ICU who did or did not survive COVID-19. Right: quantification of the data across all infected ICU individuals. *$p < 0.05$, ns as determined by a Student's unpaired t test.

(B) SARS-CoV-2-specific $CD8^+$ T cells from non-survivors produce elevated levels of IL-6. Left: pseudocolor plots of baseline and spike-stimulated samples from the two individuals harboring the highest levels of SARS-CoV-2-specific $CD8^+$ T cells in (A), only one of whom survived. Top right: histograms showing expression levels of IL-6 in non-survivor and survivor $CD8^+$ T cells. Bottom right: proportion of IL-6-producing cells among total and SARS-CoV-2-specific T cells in all non-survivors and survivors.

(C) Positive control for IL-6 detection. Peripheral blood monocytes ($CD3^-CD4^{dim}$ cells) were stimulated with LPS and analyzed by CyTOF.

(D) SARS-CoV-2-specific Treg cells, but not cTfh cells, are significantly more abundant in non-survivors of severe COVID-19.

Datapoints from graphs with significance tests correspond to individual specimens (biological replicates). See also Figures S3–S5.

disease. We also, similar to multiple other studies (Mathew et al., 2020; Rydyznski Moderbacher et al., 2020), found memory T cells to be significantly more abundant in individuals with severe disease, although this was likely due to the older age of the severe group, which affects memory cell frequencies (Rydyznski Moderbacher et al., 2020).

Among SARS-CoV-2-specific cells, $CD4^+$ Tem cells were increased in severe cases, but $CD4^+$ Temra cells were markedly depleted. The biological significance of this difference is unclear because both Tem and Temra cells can play important roles in antiviral immunity (Dunne et al., 2002; Lilleri et al., 2008; Northfield et al., 2007; Sridhar et al., 2013; Weiskopf et al., 2015). SARS-CoV-2-specific cTfh cells were also more abundant in moderate and severe cases, and this paralleled a corresponding increase in total cTfh cells in more severe cases, the latter of which has been reported previously (Oja et al., 2020).

T cell exhaustion, as defined by the exhaustion marker PD1, was reported early during the pandemic (De Biasi et al., 2020; Diao et al., 2020), but a recent study suggested that $PD1^+$ $CD8^+$ T cells from individuals recovering from COVID-19 can be functional and that PD1 may more often represent an activation marker in these individuals (Rha et al., 2021). We therefore looked within our datasets for features of T cell exhaustion among our total and SARS-CoV-2-specific cells. We defined exhausted cells as those dually expressing elevated PD1 and TIGIT or PD1 and CTLA4. In both instances, we found a significant increase in exhausted SARS-CoV-2-specific T cells in severe cases. These results, together with the finding that T cells from hospitalized individuals activated by SARS-CoV-2 peptide stimulation express elevated transcript levels of multiple exhaustion markers (PD1, TIGIT, LAG3, and TIM3) relative to those from non-hospitalized individuals (Meckiff et al., 2020), suggest that T cell exhaustion correlates with disease severity. We also observed co-expression of PD1 with the Fas receptor CD95, involved in apoptosis, and that $PD1^+CD95^+$ T cells within the total and SARS-CoV-2-specific compartments were elevated in severe relative to mild cases. These observations are in line with upregulation of CD95 transcripts on total T cells during

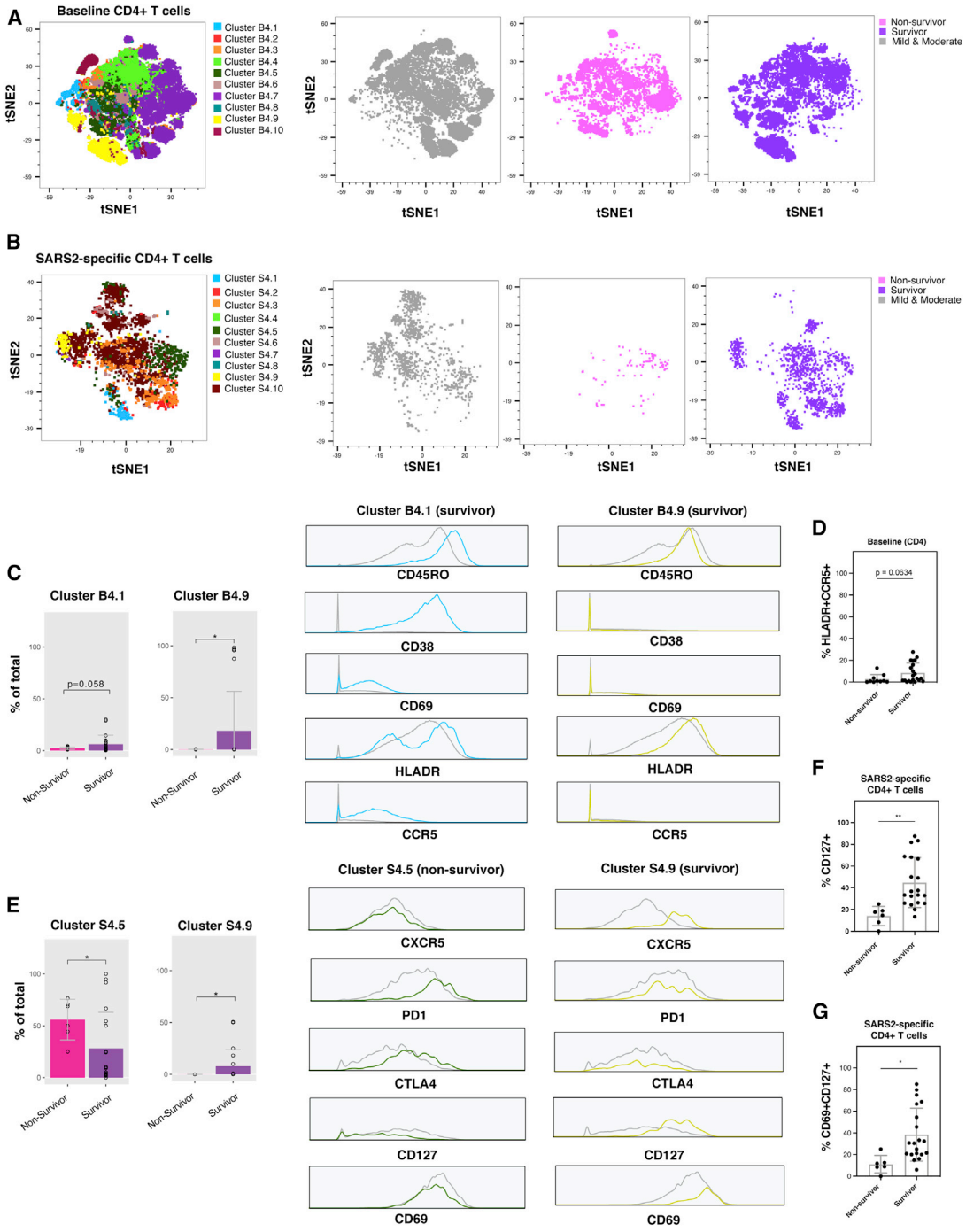

Figure 6. Clustering reveals enrichment of long-lived, activated SARS-CoV-2-specific CD4$^+$ T cells in individuals who successfully recover from severe COVID-19

(A and B) The phenotypes of total (A) and SARS-CoV-2-specific (B) CD4$^+$ T cells differ between non-survivors and survivors of severe COVID-19. Left: t-SNE plot and FlowSOM clusters identified in Figures 3A (A) and 3C (B). Right: distribution of CD4$^+$ T cells from non-survivors (pink), survivors (purple), and mild and moderate groups (gray).

(C) Activated memory CD4$^+$ T cells are elevated in survivors of severe COVID-19. Left: clusters B4.1 and B4.9 are enriched in the survivor relative to the non-survivor group. *$p < 0.05$ as determined by a Student's unpaired t test. Right: cells from clusters B4.1 and B4.9 are memory (CD45RO$^+$) cells and express elevated levels of the activation marker HLADR. Other activation markers (CD38, CD69, and CCR5) are preferentially elevated only in cluster B4.1. Expression levels are displayed in gray for total CD4$^+$ T cells and in color for clusters.

(D) Survivors tend to harbor more activated (HLADR$^+$CCR5$^+$) CD4$^+$ T cells.

(legend continued on next page)

COVID-19 (Zhu et al., 2020) and with reports of apoptotic T cells during severe (Yao et al., 2021) and fatal (Feng et al., 2020) COVID-19, during which elevated CD95 was observed in the dying cells. Together, these results suggest increased proportions of exhausted and apoptosis-prone T cells during severe COVID-19.

SARS-CoV-2-specific T cell frequency predicts survival from severe COVID-19

To our knowledge, this is the first study to directly compare, via in-depth immune phenotyping, the features of T cells from individuals with severe (ICU) COVID-19 who do versus do not survive disease. We discovered in a cross-sectional analysis that survivors mounted a higher SARS-CoV-2-specific T cell response, and longitudinal analyses revealed that this response increases in survivors prior to recovery whereas it does not in non-survivors. These data suggest that SARS-CoV-2-specific T cells are protective during severe COVID-19 and are in line with a number of other reports, including: a recent report of greater expansion of SARS-CoV-2-specific T cells during moderate than severe COVID-19 (Liao et al., 2020); the finding that antigen-specific T cells against SARS-CoV-1, a close relative of SARS-CoV-2, are protective in mouse infection models (Zhao et al., 2016); and a recent study demonstrating SARS-CoV-2-specific T cell responses, as defined by AIM markers, to be associated with less severe disease (Rydyznski Moderbacher et al., 2020). Although the latter study did not focus on fatal versus non-fatal outcomes, it included one fatal case with longitudinal sampling and observed that individual to have had no detectable SARS-CoV-2-specific T cell responses 16 and 11 days prior to death, in line with our findings. The data are consistent with the notion of SARS-CoV-2-specific T cells being beneficial rather than detrimental for surviving severe COVID-19. That being said, we did find that SARS-CoV-2-specific $CD8^+$ T cells co-producing IFNγ and IL-6 were elevated in individuals who did not survive severe disease. Plasma IL-6 levels are associated with COVID-19 severity (Huang et al., 2020; Mathew et al., 2020; Zhou et al., 2020a) and predict COVID-19-associated death (Del Valle et al., 2020). However, except for a study that reported elevated IL-6 production in total $CD4^+$ T cells from individuals with COVID-19 in the ICU (Zhou et al., 2020b), IL-6 is not thought to be produced by T cells during SARS-CoV-2 infection. Whether IL-6 production by SARS-CoV-2-specific $CD8^+$ T cells directly contributes to immunopathogenesis remains to be determined.

Potential mechanisms underlying diminished SARS-CoV-2-specific T cell responses in non-survivors of severe COVID-19

Our data suggest multiple mechanisms by which individuals with severe disease may control production of SARS-CoV-2-specific T cells. Hospitalized individuals who produced few SARS-CoV-2-specific T cells—and were more likely to die—harbored higher frequencies of SARS-CoV-2-specific Treg cells. Although little is known about SARS-CoV-2-specific Treg cells, the proportion of Treg cells among total T cells has been reported to be both increased (De Biasi et al., 2020) and decreased (Qin et al., 2020) during severe COVID-19. Consistent with increased levels of Treg cells during severe infection are observations of disease severity positively associating with levels of IL-10, a regulatory cytokine commonly produced by Treg cells (Han et al., 2020; Zhao et al., 2020b). We did not observe increased levels of total Treg cells in fatal versus non-fatal cases of severe COVID-19, but the increased number of SARS-CoV-2-specific Treg cells in non-survivors may suffice to hinder differentiation of SARS-CoV-2-specific effector T cells.

Our finding may seem at odds with a recent study suggesting a decrease in SARS-CoV-2-specific Treg cells during severe disease (Meckiff et al., 2020). However, differences in experimental design likely account for the differences. Our study compared individuals in the ICU who survived with those who did not survive, and the other study compared individuals in the ICU with non-hospitalized ones. Furthermore, the prior study identified SARS-CoV-2-specific Treg cells as those expressing AIM markers after stimulation for 24 h with SARS-CoV-2 peptides, whereas we identified the cells as those producing IFNγ after 6 h of stimulation. Because all the SARS-CoV-2-specific cells characterized in our study were defined based on IFNγ induction, the SARS-CoV-2-specific Treg cells we identified are, in fact, a subset of all possible Treg cells. These IFNγ^+ Treg cells have been reported to play important roles during graft rejection and autoimmunity (Daniel et al., 2008; McClymont et al., 2011) but, to our knowledge, have not been described during viral infection.

Another potential mechanism accounting for increased frequencies of SARS-CoV-2-specific T cells in survivors is their harboring increased expression of CD127, a component of the IL-7 receptor complex important for homeostatic proliferation. We recently demonstrated that SARS-CoV-2-specific T cells from convalescent individuals proliferate homeostatically in response to IL-7 (Neidleman et al., 2020a). We speculate that, during severe COVID-19, elevated expression of CD127 allows SARS-CoV-2-specific T cells to expand more rapidly and persist in sufficient quantities to aid recovery.

CXCR4 antagonism as a target for T cell-mediated immunopathogenesis in the lungs

One of the most interesting findings of this study resulted from our analysis of longitudinal specimens from fatal versus non-fatal severe cases, where we found $CXCR4^+CD69^+$ T cells decreasing over time in those who survived and increasing in those who did

(E) Left: cluster S4.5 is enriched in non-survivors and cluster S4.9 in survivors. Right: cells from cluster S4.5 co-express the exhaustion markers PD1 and CTLA4, whereas cells from cluster S4.9 express high levels of the cTfh marker CXCR5, low levels of the exhaustion markers PD1 and CTLA4, high levels of IL-7 receptor alpha chain CD127, and high levels of the activation marker CD69. Expression levels from each cluster (colored traces) are shown against expression levels from all SARS-CoV-2-specific $CD4^+$ T cell clusters combined (gray traces). *$p < 0.05$ as determined by a Student's unpaired t test.
(F and G) SARS-CoV-2-specific $CD4^+$ T cells expressing CD127 (F) or co-expressing CD127 with CD69 (G) are more abundant in survivors than in non-survivors. *$p < 0.05$, **$p < 0.01$, as determined by a Student's unpaired t test.
Datapoints from graphs with significance tests correspond to individual specimens (biological replicates). See also Figures S6 and S7.

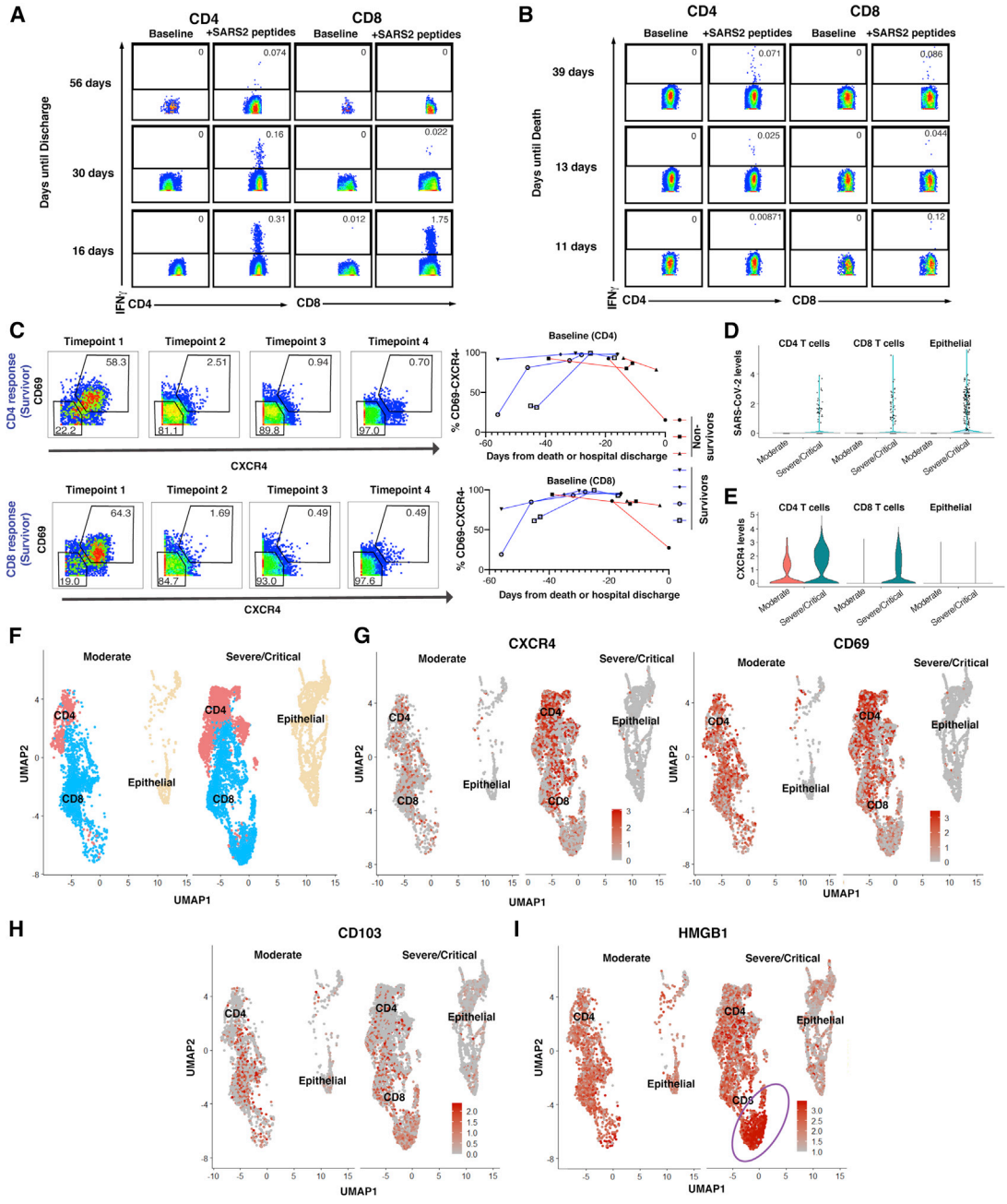

Figure 7. Escalating numbers of SARS-CoV-2-specific and diminishing numbers of lung-homing bystander CXCR4$^+$ T cells correlate with survival of severe COVID-19

(A and B) Longitudinal analysis of an individual who survived (A) and did not survive (B) severe COVID-19, demonstrating an increasing number of SARS-CoV-2 T cells producing IFNγ over time in the survivor but not in the non-survivor.

(C) Activated CXCR4-expressing T cells decrease over time in survivors but not in the non-survivors. Left: pseudocolor plots showing gating for CD69$^+$CXCR4$^+$ and CD69$^-$CXCR4$^-$ cells among total CD4$^+$ and CD8$^+$ T cells in longitudinal specimens from a representative survivor of severe COVID-19. Right: longitudinal analyses of 7 cases of severe COVID-19, 4 of which survived infection. Although the frequencies of CXCR4$^-$CD69$^-$ T cells increase over time in survivors (blue lines), they decrease over time in non-survivors (red lines).

(D–I) Higher levels of infiltrating CXCR4$^+$CD69$^+$ T cells are present in lungs of individuals with severe/critical versus moderate COVID-19, as determined by mining of public BAL scRNA-seq datasets. Higher levels of SARS-CoV-2 viral reads in T and epithelial cells were detected during severe COVID-19 (D), which were also

(legend continued on next page)

not. CXCR4 plays important roles in lymphocyte chemotaxis and in homing of hematopoietic stem cells to the bone marrow. Its primary ligand, CXCL12, is expressed in multiple tissues but of importance for this study, is elevated in damaged lungs, particularly the lung vasculature (Mamazhakypov et al., 2021). Interestingly, $CD69^{+}CXCR4^{+}$ T cells have been found at elevated levels in non-small cell lung cancer tissues compared with normal lung tissue (Wald et al., 2006), suggesting their increased presence under pathologic conditions. Indeed, we found that T cells expressing CXCR4 and CD69 are elevated in BAL fluid of individuals with severe COVID-19. These cells likely migrated from the periphery because they express low levels of the Trm marker CD103. Consistent with an infiltration of pathogenic T cells during severe COVID-19 are observations that pulmonary T cells during critical compared with moderate disease expressed fewer tissue-resident transcripts (Liao et al., 2020) and proteins (Oja et al., 2020). Trm cells may, however, play a role in pathogenesis by producing the CXCR4 ligand HMGB1, which, consistent with our findings, has been reported to be elevated during fatal COVID-19 (Chen et al., 2020b).

Together with the observation of activation of CMV- and EBV-specific T cells during the acute phase of COVID-19 (Sekine et al., 2020), these findings bring up the possibility that, during critical and fatal COVID-19, T cells in the periphery activated through bystander effects are recruited to the lungs via CXCR4-mediated chemotaxis, and this contributes to pulmonary damage. If CXCR4-driven T cell infiltration does indeed contribute to fatal COVID-19, then inhibitors against this receptor may be useful. AMD3100, a CXCR4 antagonist that has been used to mobilize stem cells (Cashen et al., 2007), could be tested in clinical trials. Optimized derivatives of a peptide called EPI-X4, originally discovered because of its ability to inhibit CXCR4-tropic HIV infection of target cells (Zirafi et al., 2015), exhibit superior activity over AMD3100 for blocking CXCR4-mediated chemotaxis and have been shown to potently block migration of immune cells into the lungs of asthmatic mice (Harms et al., 2020). These derivatives are intriguing candidates for treatment of severe COVID-19.

Conclusions

Our findings overall support a beneficial rather than immunopathologic role of effector SARS-CoV-2-specific T cells during severe acute infection. This was evidenced by survivors of severe infection exhibiting (1) escalating SARS-CoV-2-specific T cell numbers before recovery, (2) increased levels of SARS-CoV-2-specific T cells with homeostatic proliferative potential, and (3) diminished numbers of immunosuppressive SARS-CoV-2-specific Treg cells. The mechanisms by which T cells would help recovery from severe infection are not clear but likely involve providing B cell help and direct cytolysis of infected cells. In addition, because IFNγ downregulates ACE2 (de Lang et al., 2006), production of this cytokine by SARS-CoV-2-specific T cells may limit the availability of host cells for the virus. Exceptions to the notion of "beneficial" T cells, however, are our observations of non-survivors expressing elevated levels of IL-6-producing SARS-CoV-2-specific $CD8^{+}$ T cells and the increase of activated, lung-homing bystander T cells in the days leading up to death. Nevertheless, taking into consideration the longevity of SARS-CoV-2-specific T cells (Zuo et al., 2021), our results suggest that strategies to boost the effector functions of SARS-CoV-2-specific T cells, including by vaccination, will be beneficial for decreasing COVID-19 mortality and helping to end this devastating pandemic.

Limitations of the study

Our study has limitations. To enable deep phenotyping of SARS-CoV-2-specific T cells, we had to characterize a relatively small cohort of 34 infected individuals. This may have accounted for our inability to detect sex-based differences. Future studies should confirm, in larger cohorts, the findings reported here. Such studies should account for the racial, social, and demographic factors that can influence immune responses to SARS-CoV-2. A second limitation was our use of peptide stimulation to identify SARS-CoV-2-specific cells. To try to minimize phenotypic changes associated with *ex vivo* cognate peptide encounter, we limited the stimulation to 6 h; we acknowledge, however, that the phenotypes of our SARS-CoV-2-specific T cells correspond to those immediately following antigen encounter rather than at baseline. Importantly, we did not compare the phenotypes of baseline cells with SARS-CoV-2-specific ones; such a comparison would include artifacts resulting from the stimulation. Instead, we always compared SARS-CoV-2-specific T cells between different groups of individuals. A third limitation was our restricting analysis of SARS-CoV-2-specific T cells to those recognizing the spike protein, which elicits a limited $CD8^{+}$ T cell response. Future studies should examine responses against proteins more commonly recognized by SARS-CoV-2-specific $CD8^{+}$ T cells (Ferretti et al., 2020). Fourth, this study was a phenotyping and correlative study, so follow-up functional assays, including testing the effects of interventions *in vivo*, will be required to establish cause versus effect. Finally, our CyTOF analysis was limited to cells from the blood, although we confirmed the presence of activated $CXCR4^{+}$ T cells in the lungs of individuals with severe COVID-19.

STAR★METHODS

Detailed methods are provided in the online version of this paper and include the following:

- KEY RESOURCES TABLE
- RESOURCE AVAILABILITY
  - Lead contact
  - Materials availability
  - Data and code availability

associated with higher levels of CXCR4 in T cells, as depicted by violin plots (E). Viral reads detected in T cells likely reflect cell surface virion sticking because these cells do not express ACE2. UMAP visualization of T and epithelial cells from the scRNA-seq datasets (F) revealed elevated expression of CXCR4 and CD69 on subsets of T cells (G) separate from T cells expressing high levels of the Trm marker CD103 (H). The CXCR4 ligand HMGB1 was expressed in T and epithelial cells but especially concentrated among a subset of $CXCR4^{-}CD69^{-}$ Trm $CD8^{+}$ T cells outlined in purple (I).
See also Figure S8.

SUPPLEMENTAL INFORMATION

Supplemental information can be found online at https://doi.org/10.1016/j.celrep.2021.109414.

ACKNOWLEDGMENTS

This work was supported by the Van Auken Private Foundation, David Henke, and Pamela and Edward Taft (to N.R.R.); the Program for Breakthrough Biomedical Research (to N.R.R., E.G., S.A.L., and J.V.), which is partly funded by the Sandler Foundation; philanthropic funds to Gladstone by The Roddenberry Foundation (to N.R.R.); awards 2164 (to N.R.R.), 2208 (to N.R.R.), and 2160 (to S.A.L.) from Fast Grants; and NIH R01 AI123126-05S1 (to E.G.). We acknowledge NIH DRC Center grant P30 DK063720 and S10 1S10OD018040 for use of CyTOF. We thank S. Tamaki, T. Peech, and C. Bispo for CyTOF assistance; H. Hartig for recruitment; N. Lazarus and E. Butcher for Act1; J. Carroll for graphics; F. Chanut for editorial assistance; and R. Givens for administrative assistance.

AUTHOR CONTRIBUTIONS

J.N., A.F.G., and M.M. performed experiments and conducted data analyses. X.L. and J.Y. conducted data analyses. C.Y. collected specimens and performed experiments. V.M. and G.G. enrolled participants and collected specimens. W.C.G. participated in analysis and supervised. J.V. conceived ideas for the study. S.A.L. established CHIRP and supervised. E.G. conceived ideas for the study, analyzed data, and supervised. K.L.L. provided specimens, analyzed data, and supervised. N.R.R. conceived ideas for the study, analyzed data, supervised, and wrote the manuscript.

DECLARATION OF INTERESTS

The authors declare no competing financial interests.

Received: February 26, 2021
Revised: May 14, 2021
Accepted: June 24, 2021
Published: June 29, 2021

REFERENCES

Anft, M., Paniskaki, K., Blazquez-Navarro, A., Doevelaar, A., Seibert, F.S., Hoelzer, B., Skrzypczyk, S., Kohut, E., Kurek, J., Zapka, J., et al. (2020). COVID-19 progression is potentially driven by T cell immunopathogenesis. medRxiv. https://doi.org/10.1101/2020.04.28.20083089.

Bastard, P., Rosen, L.B., Zhang, Q., Michailidis, E., Hoffmann, H.H., Zhang, Y., Dorgham, K., Philippot, Q., Rosain, J., Béziat, V., et al.; HGID Lab; NIAID-USUHS Immune Response to COVID Group; COVID Clinicians; COVID-STORM Clinicians; Imagine COVID Group; French COVID Cohort Study Group; Milieu Intérieur Consortium; CoV-Contact Cohort; Amsterdam UMC Covid-19 Biobank; COVID Human Genetic Effort (2020). Autoantibodies against type I IFNs in patients with life-threatening COVID-19. Science *370*, eabd4585.

Braun, J., Loyal, L., Frentsch, M., Wendisch, D., Georg, P., Kurth, F., Hippenstiel, S., Dingeldey, M., Kruse, B., Fauchere, F., et al. (2020). SARS-CoV-2-reactive T cells in healthy donors and patients with COVID-19. Nature *587*, 270–274.

Cashen, A.F., Nervi, B., and DiPersio, J. (2007). AMD3100: CXCR4 antagonist and rapid stem cell-mobilizing agent. Future Oncol. *3*, 19–27.

Cavrois, M., Banerjee, T., Mukherjee, G., Raman, N., Hussien, R., Rodriguez, B.A., Vasquez, J., Spitzer, M.H., Lazarus, N.H., Jones, J.J., et al. (2017). Mass Cytometric Analysis of HIV Entry, Replication, and Remodeling in Tissue CD4+ T Cells. Cell Rep. *20*, 984–998.

Chen, G., Wu, D., Guo, W., Cao, Y., Huang, D., Wang, H., Wang, T., Zhang, X., Chen, H., Yu, H., et al. (2020a). Clinical and immunological features of severe and moderate coronavirus disease 2019. J. Clin. Invest. *130*, 2620–2629.

Chen, L., Long, X., Xu, Q., Tan, J., Wang, G., Cao, Y., Wei, J., Luo, H., Zhu, H., Huang, L., et al. (2020b). Elevated serum levels of S100A8/A9 and HMGB1 at hospital admission are correlated with inferior clinical outcomes in COVID-19 patients. Cell. Mol. Immunol. *17*, 992–994.

Daniel, V., Naujokat, C., Sadeghi, M., Weimer, R., Renner, F., Yildiz, S., and Opelz, G. (2008). Observational support for an immunoregulatory role of CD3+CD4+CD25+IFN-gamma+ blood lymphocytes in kidney transplant recipients with good long-term graft outcome. Transpl. Int. *21*, 646–660.

De Biasi, S., Meschiari, M., Gibellini, L., Bellinazzi, C., Borella, R., Fidanza, L., Gozzi, L., Iannone, A., Lo Tartaro, D., Mattioli, M., et al. (2020). Marked T cell activation, senescence, exhaustion and skewing towards TH17 in patients with COVID-19 pneumonia. Nat. Commun. *11*, 3434.

de Lang, A., Osterhaus, A.D., and Haagmans, B.L. (2006). Interferon-gamma and interleukin-4 downregulate expression of the SARS coronavirus receptor ACE2 in Vero E6 cells. Virology *353*, 474–481.

Del Valle, D.M., Kim-Schulze, S., Huang, H.H., Beckmann, N.D., Nirenberg, S., Wang, B., Lavin, Y., Swartz, T.H., Madduri, D., Stock, A., et al. (2020). An inflammatory cytokine signature predicts COVID-19 severity and survival. Nat. Med. *26*, 1636–1643.

Diao, B., Wang, C., Tan, Y., Chen, X., Liu, Y., Ning, L., Chen, L., Li, M., Liu, Y., Wang, G., et al. (2020). Reduction and Functional Exhaustion of T Cells in Patients With Coronavirus Disease 2019 (COVID-19). Front. Immunol. *11*, 827.

Dobin, A., Davis, C.A., Schlesinger, F., Drenkow, J., Zaleski, C., Jha, S., Batut, P., Chaisson, M., and Gingeras, T.R. (2013). STAR: ultrafast universal RNA-seq aligner. Bioinformatics *29*, 15–21.

Docherty, A.B., Harrison, E.M., Green, C.A., Hardwick, H.E., Pius, R., Norman, L., Holden, K.A., Read, J.M., Dondelinger, F., Carson, G., et al.; ISARIC4C investigators (2020). Features of 20 133 UK patients in hospital with covid-19 using the ISARIC WHO Clinical Characterisation Protocol: prospective observational cohort study. BMJ *369*, m1985.

Dunne, P.J., Faint, J.M., Gudgeon, N.H., Fletcher, J.M., Plunkett, F.J., Soares, M.V., Hislop, A.D., Annels, N.E., Rickinson, A.B., Salmon, M., and Akbar, A.N. (2002). Epstein-Barr virus-specific CD8(+) T cells that re-express CD45RA are apoptosis-resistant memory cells that retain replicative potential. Blood *100*, 933–940.

Feng, Z., Diao, B., Wang, R., Wang, G., Wang, C., Tan, Y., Liu, L., Wang, C., Liu, Y., Yuan, Z., et al. (2020). The Novel Severe Acute Respiratory Syndrome Coronavirus 2 (SARS-CoV-2) Directly Decimates Human Spleens and Lymph Nodes. medRxiv. https://doi.org/10.1101/2020.03.27.20045427.

Ferretti, A.P., Kula, T., Wang, Y., Nguyen, D.M.V., Weinheimer, A., Dunlap, G.S., Xu, Q., Nabilsi, N., Perullo, C.R., Cristofaro, A.W., et al. (2020). Unbiased Screens Show CD8$^+$ T Cells of COVID-19 Patients Recognize Shared Epitopes in SARS-CoV-2 that Largely Reside outside the Spike Protein. Immunity *53*, 1095–1107.e3.

Garcia-Beltran, W.F., Lam, E.C., Astudillo, M.G., Yang, D., Miller, T.E., Feldman, J., Hauser, B.M., Caradonna, T.M., Clayton, K.L., Nitido, A.D., et al. (2021). COVID-19 neutralizing antibodies predict disease severity and survival. Cell *184*, 476–488.

Grasselli, G., Zangrillo, A., Zanella, A., Antonelli, M., Cabrini, L., Castelli, A., Cereda, D., Coluccello, A., Foti, G., Fumagalli, R., et al.; COVID-19 Lombardy ICU Network (2020). Baseline Characteristics and Outcomes of 1591 Patients

Infected With SARS-CoV-2 Admitted to ICUs of the Lombardy Region, Italy. JAMA *323*, 1574–1581.

Grifoni, A., Weiskopf, D., Ramirez, S.I., Mateus, J., Dan, J.M., Moderbacher, C.R., Rawlings, S.A., Sutherland, A., Premkumar, L., Jadi, R.S., et al. (2020). Targets of T Cell Responses to SARS-CoV-2 Coronavirus in Humans with COVID-19 Disease and Unexposed Individuals. Cell *181*, 1489–1501.e15.

Han, H., Ma, Q., Li, C., Liu, R., Zhao, L., Wang, W., Zhang, P., Liu, X., Gao, G., Liu, F., et al. (2020). Profiling serum cytokines in COVID-19 patients reveals IL-6 and IL-10 are disease severity predictors. Emerg. Microbes Infect. *9*, 1123–1130.

Harms, M., Habib, M.M.W., Nemska, S., Nicolo, A., Gilg, A., Preising, N., Sokkar, P., Carmignani, S., Raasholm, M., Weidinger, G., et al. (2020). An optimized derivative of an endogenous CXCR4 antagonist prevents atopic dermatitis and airway inflammation. Acta Pharm. Sin. B, Published online December 13, 2020. https://doi.org/10.1016/j.apsb.2020.12.005.

Hotez, P.J., Bottazzi, M.E., and Corry, D.B. (2020). The potential role of Th17 immune responses in coronavirus immunopathology and vaccine-induced immune enhancement. Microbes Infect. *22*, 165–167.

Huang, C., Wang, Y., Li, X., Ren, L., Zhao, J., Hu, Y., Zhang, L., Fan, G., Xu, J., Gu, X., et al. (2020). Clinical features of patients infected with 2019 novel coronavirus in Wuhan, China. Lancet *395*, 497–506.

Ito, T., Carson, W.F., 4th, Cavassani, K.A., Connett, J.M., and Kunkel, S.L. (2011). CCR6 as a mediator of immunity in the lung and gut. Exp. Cell Res. *317*, 613–619.

Liao, M., Liu, Y., Yuan, J., Wen, Y., Xu, G., Zhao, J., Cheng, L., Li, J., Wang, X., Wang, F., et al. (2020). Single-cell landscape of bronchoalveolar immune cells in patients with COVID-19. Nat. Med. *26*, 842–844.

Lilleri, D., Fornara, C., Revello, M.G., and Gerna, G. (2008). Human cytomegalovirus-specific memory CD8+ and CD4+ T cell differentiation after primary infection. J. Infect. Dis. *198*, 536–543.

Liu, L., Wei, Q., Lin, Q., Fang, J., Wang, H., Kwok, H., Tang, H., Nishiura, K., Peng, J., Tan, Z., et al. (2019). Anti-spike IgG causes severe acute lung injury by skewing macrophage responses during acute SARS-CoV infection. JCI Insight *4*, e123158.

Lynch, K.L., Whitman, J.D., Lacanienta, N.P., Beckerdite, E.W., Kastner, S.A., Shy, B.R., Goldgof, G.M., Levine, A.G., Bapat, S.P., Stramer, S.L., et al. (2021). Magnitude and kinetics of anti-SARS-CoV-2 antibody responses and their relationship to disease severity. Clin. Infect. Dis. *72*, 301–308.

Ma, T., Luo, X., George, A.F., Mukherjee, G., Sen, N., Spitzer, T.L., Giudice, L.C., Greene, W.C., and Roan, N.R. (2020). HIV efficiently infects T cells from the endometrium and remodels them to promote systemic viral spread. eLife *9*, e55487.

Mamazhakypov, A., Viswanathan, G., Lawrie, A., Schermuly, R.T., and Rajagopal, S. (2021). The role of chemokines and chemokine receptors in pulmonary arterial hypertension. Br. J. Pharmacol. *178*, 72–89.

Mathew, D., Giles, J.R., Baxter, A.E., Oldridge, D.A., Greenplate, A.R., Wu, J.E., Alanio, C., Kuri-Cervantes, L., Pampena, M.B., D'Andrea, K., et al.; UPenn COVID Processing Unit (2020). Deep immune profiling of COVID-19 patients reveals distinct immunotypes with therapeutic implications. Science *369*, eabc8511.

McClymont, S.A., Putnam, A.L., Lee, M.R., Esensten, J.H., Liu, W., Hulme, M.A., Hoffmüller, U., Baron, U., Olek, S., Bluestone, J.A., and Brusko, T.M. (2011). Plasticity of human regulatory T cells in healthy subjects and patients with type 1 diabetes. J. Immunol. *186*, 3918–3926.

Meckiff, B.J., Ramirez-Suastegui, C., Fajardo, V., Chee, S.J., Kusnadi, A., Simon, H., Grifoni, A., Pelosi, E., Weiskopf, D., Sette, A., et al. (2020). Single-cell transcriptomic analysis of SARS-CoV-2 reactive CD4 (+) T cells. bioRxiv. https://doi.org/10.1101/2020.06.12.148916.

Neidleman, J., Luo, X., Frouard, J., Xie, G., Gill, G., Stein, E.S., McGregor, M., Ma, T., George, A.F., Kosters, A., et al. (2020a). SARS-CoV-2-Specific T Cells Exhibit Phenotypic Features of Helper Function, Lack of Terminal Differentiation, and High Proliferation Potential. Cell Rep Med *1*, 100081.

Neidleman, J., Luo, X., Frouard, J., Xie, G., Hsiao, F., Ma, T., Morcilla, V., Lee, A., Telwatte, S., Thomas, R., et al. (2020b). Phenotypic analysis of the unstimulated in vivo HIV CD4 T cell reservoir. eLife *9*, e55487.

Northfield, J.W., Loo, C.P., Barbour, J.D., Spotts, G., Hecht, F.M., Klenerman, P., Nixon, D.F., and Michaëlsson, J. (2007). Human immunodeficiency virus type 1 (HIV-1)-specific CD8+ T(EMRA) cells in early infection are linked to control of HIV-1 viremia and predict the subsequent viral load set point. J. Virol. *81*, 5759–5765.

Oja, A.E., Saris, A., Ghandour, C.A., Kragten, N.A.M., Hogema, B.M., Nossent, E.J., Heunks, L.M.A., Cuvalay, S., Slot, E., Linty, F., et al. (2020). Divergent SARS-CoV-2-specific T- and B-cell responses in severe but not mild COVID-19 patients. Eur. J. Immunol. *50*, 1998–2012.

Pacha, O., Sallman, M.A., and Evans, S.E. (2020). COVID-19: a case for inhibiting IL-17? Nat. Rev. Immunol. *20*, 345–346.

Qin, C., Zhou, L., Hu, Z., Zhang, S., Yang, S., Tao, Y., Xie, C., Ma, K., Shang, K., Wang, W., and Tian, D.S. (2020). Dysregulation of Immune Response in Patients With Coronavirus 2019 (COVID-19) in Wuhan, China. Clin. Infect. Dis. *71*, 762–768.

Rha, M.S., Jeong, H.W., Ko, J.H., Choi, S.J., Seo, I.H., Lee, J.S., Sa, M., Kim, A.R., Joo, E.J., Ahn, J.Y., et al. (2021). PD-1-Expressing SARS-CoV-2-Specific CD8(+) T Cells Are Not Exhausted, but Functional in Patients with COVID-19. Immunity *54*, 44–52.e3.

Rydyznski Moderbacher, C., Ramirez, S.I., Dan, J.M., Grifoni, A., Hastie, K.M., Weiskopf, D., Belanger, S., Abbott, R.K., Kim, C., Choi, J., et al. (2020). Antigen-Specific Adaptive Immunity to SARS-CoV-2 in Acute COVID-19 and Associations with Age and Disease Severity. Cell *183*, 996–1012.e19.

Schiraldi, M., Raucci, A., Muñoz, L.M., Livoti, E., Celona, B., Venereau, E., Apuzzo, T., De Marchis, F., Pedotti, M., Bachi, A., et al. (2012). HMGB1 promotes recruitment of inflammatory cells to damaged tissues by forming a complex with CXCL12 and signaling via CXCR4. J. Exp. Med. *209*, 551–563.

Sekine, T., Perez-Potti, A., Rivera-Ballesteros, O., Strålin, K., Gorin, J., Olsson, A., Llewellyn-Lacey, S., Kamal, H, Bogdanovic, G., Muschiol, S., et al. (2020). Robust T cell immunity in convalescent individuals with asymptomatic or mild COVID-19. Cell *183*, 158–168.e14.

Sorci, G., Faivre, B., and Morand, S. (2020). Explaining among-country variation in COVID-19 case fatality rate. Sci. Rep. *10*, 18909.

Soresina, A., Moratto, D., Chiarini, M., Paolillo, C., Baresi, G., Focà, E., Bezzi, M., Baronio, B., Giacomelli, M., and Badolato, R. (2020). Two X-linked agammaglobulinemia patients develop pneumonia as COVID-19 manifestation but recover. Pediatr. Allergy Immunol. *31*, 565–569.

Sridhar, S., Begom, S., Bermingham, A., Hoschler, K., Adamson, W., Carman, W., Bean, T., Barclay, W., Deeks, J.J., and Lalvani, A. (2013). Cellular immune correlates of protection against symptomatic pandemic influenza. Nat. Med. *19*, 1305–1312.

Stuart, T., Butler, A., Hoffman, P., Hafemeister, C., Papalexi, E., Mauck, W.M., 3rd, Hao, Y., Stoeckius, M., Smibert, P., and Satija, R. (2019). Comprehensive Integration of Single-Cell Data. Cell *177*, 1888–1902.e21.

Takahashi, T., Ellingson, M.K., Wong, P., Israelow, B., Lucas, C., Klein, J., Silva, J., Mao, T., Oh, J.E., Tokuyama, M., et al.; Yale IMPACT Research Team (2020). Sex differences in immune responses that underlie COVID-19 disease outcomes. Nature *588*, 315–320.

Thieme, C.J., Anft, M., Paniskaki, K., Blazquez-Navarro, A., Dovelaar, A., Seibert, F.S., Holzer, B., Konik, M.J., Brenner, T., Tempfer, C., et al. (2020). The SARS-CoV-2 T-cell immunity is directed against the spike, membrane, and nucleocapsid protein and associated with COVID 19 severity. Cell Rep. Med. *1*, 100092.

van der Made, C.I., Simons, A., Schuurs-Hoeijmakers, J., van den Heuvel, G., Mantere, T., Kersten, S., van Deuren, R.C., Steehouwer, M., van Reijmersdal, S.V., Jaeger, M., et al. (2020). Presence of Genetic Variants Among Young Men With Severe COVID-19. JAMA *324*, 663–673.

Van Gassen, S., Callebaut, B., Van Helden, M.J., Lambrecht, B.N., Demeester, P., Dhaene, T., and Saeys, Y. (2015). FlowSOM: Using self-organizing maps for visualization and interpretation of cytometry data. Cytometry A *87*, 636–645.

Wald, O., Izhar, U., Amir, G., Avniel, S., Bar-Shavit, Y., Wald, H., Weiss, I.D., Galun, E., and Peled, A. (2006). CD4+CXCR4highCD69+ T cells accumulate in lung adenocarcinoma. J. Immunol. *177*, 6983–6990.

Weiskopf, D., Bangs, D.J., Sidney, J., Kolla, R.V., De Silva, A.D., de Silva, A.M., Crotty, S., Peters, B., and Sette, A. (2015). Dengue virus infection elicits highly polarized CX3CR1+ cytotoxic CD4+ T cells associated with protective immunity. Proc. Natl. Acad. Sci. USA *112*, E4256–E4263.

Woodruff, M.C., Ramonell, R.P., Nguyen, D.C., Cashman, K.S., Saini, A.S., Haddad, N.S., Ley, A.M., Kyu, S., Howell, J.C., Ozturk, T., et al. (2020). Extrafollicular B cell responses correlate with neutralizing antibodies and morbidity in COVID-19. Nat. Immunol. *21*, 1506–1516.

Yao, C., Bora, S.A., Parimon, T., Zaman, T., Friedman, O.A., Palatinus, J.A., Surapaneni, N.S., Matusov, Y.P., Cerro Chiang, G., Kassar, A.G., et al. (2021). Cell-Type-Specific Immune Dysregulation in Severely Ill COVID-19 Patients. Cell Rep. *34*, 108590.

Zhang, Q., Bastard, P., Liu, Z., Le Pen, J., Moncada-Velez, M., Chen, J., Ogishi, M., Sabli, I.K.D., Hodeib, S., Korol, C., et al.; COVID-STORM Clinicians; COVID Clinicians; Imagine COVID Group; French COVID Cohort Study Group; CoV-Contact Cohort; Amsterdam UMC Covid-19 Biobank; COVID Human Genetic Effort; NIAID-USUHS/TAGC COVID Immunity Group (2020). Inborn errors of type I IFN immunity in patients with life-threatening COVID-19. Science *370*, eabd4570.

Zhao, J., Zhao, J., Mangalam, A.K., Channappanavar, R., Fett, C., Meyerholz, D.K., Agnihothram, S., Baric, R.S., David, C.S., and Perlman, S. (2016). Airway Memory CD4(+) T Cells Mediate Protective Immunity against Emerging Respiratory Coronaviruses. Immunity *44*, 1379–1391.

Zhao, Q., Meng, M., Kumar, R., Wu, Y., Huang, J., Deng, Y., Weng, Z., and Yang, L. (2020a). Lymphopenia is associated with severe coronavirus disease 2019 (COVID-19) infections: A systemic review and meta-analysis. Int. J. Infect. Dis. *96*, 131–135.

Zhao, Y., Qin, L., Zhang, P., Li, K., Liang, L., Sun, J., Xu, B., Dai, Y., Li, X., Zhang, C., et al. (2020b). Longitudinal COVID-19 profiling associates IL-1RA and IL-10 with disease severity and RANTES with mild disease. JCI Insight *5*, e139834.

Zhou, F., Yu, T., Du, R., Fan, G., Liu, Y., Liu, Z., Xiang, J., Wang, Y., Song, B., Gu, X., et al. (2020a). Clinical course and risk factors for mortality of adult inpatients with COVID-19 in Wuhan, China: a retrospective cohort study. Lancet *395*, 1054–1062.

Zhou, Y., Fu, B., Zheng, X., Wang, D., Zhao, C., Qi, Y., Sun, R., Tian, Z., Xu, X., and Wei, H. (2020b). Pathogenic T cells and inflammatory monocytes incite inflammatory storm in severe COVID-19 patients. Nat. Sci. Rev., nwaa041.

Zhu, L., Yang, P., Zhao, Y., Zhuang, Z., Wang, Z., Song, R., Zhang, J., Liu, C., Gao, Q., Xu, Q., et al. (2020). Single-Cell Sequencing of Peripheral Mononuclear Cells Reveals Distinct Immune Response Landscapes of COVID-19 and Influenza Patients. Immunity *53*, 685–696.e3.

Zirafi, O., Kim, K.A., Ständker, L., Mohr, K.B., Sauter, D., Heigele, A., Kluge, S.F., Wiercinska, E., Chudziak, D., Richter, R., et al. (2015). Discovery and characterization of an endogenous CXCR4 antagonist. Cell Rep. *11*, 737–747.

Zuo, J., Dowell, A., Pearce, H., Verma, K., Long, H.M., Begum, J., Aiano, F., Amin-Chowdhury, Z., Hallis, B., Stapley, L., et al. (2021). Robust SARS-CoV-2-specific T-cell immunity is maintained at 6 months following primary infection. Nat. Immunol. *22*, 620–626.

STAR★METHODS

KEY RESOURCES TABLE

REAGENT or RESOURCE	SOURCE	IDENTIFIER
Antibodies		
HLADR	Thermofisher	Cat#Q22158
RORγt	Fisher Scientific	Cat#5013565
CD49d (α4)	Fluidigm	Cat#3141004B
CTLA4	Fisher Scientific	Cat#5012919
NFAT	Fluidigm	Cat#3143023A
CCR5	Fluidigm	Cat#3144007A
IL5	Biolegend	Cat#504309
CD95	Fisher Scientific	Cat#MAB326100
CD7	Fluidigm	Cat#3147006B
ICOS	Fluidigm	Cat#3148019B
Tbet	Fisher Scientific	Cat#5013190
IL4	Biolegend	Cat#500829
CD2	Fluidigm	Cat#3151003B
IL17	Biolegend	Cat#512331
CD62L	Fluidigm	Cat#3153004B
TIGIT	Fludigm	Cat#3154016B
CCR6	BD Biosciences	Cat#559560
IL6	Biolegend	Cat#501115
CD8	Biolegend	Cat#301053
CD19	Biolegend	Cat#302247
CD14	Biolegend	Cat#301843
OX40	Fluidigm	Cat#3158012B
CCR7	Fluidigm	Cat#3159003A
CD28	Fluidigm	Cat#3160003B
CD45RO	Biolegend	Cat#304239
CD69	Fluidigm	Cat#3162001B
CRTH2	Fluidigm	Cat#3163003B
PD-1	Biolegend	Cat#329941
CD127	Fluidigm	Cat#3165008B
CXCR5	BD Biosciences	Cat#552032
CD27	Fluidigm	Cat#3167006B
IFNγ	Fluidigm	Cat#3168005B
CD45RA	Fluidigm	Cat#3169008B
CD3	Fluidigm	Cat#3170001B
CD57	Biolegend	Cat#359602
CD38	Fluidigm	Cat#3172007B
CD4	Fluidigm	Cat#3174004B
CXCR4	Fluidigm	Cat#3175001B
CD25	Biolegend	Cat#356102
CD161	Biolegend	Cat#339919
Purified Mouse anti-Human CD49d	BD Biosciences	Cat#340976
Purified Mouse anti-Human CD28	BD Biosciences	Cat#340975

(*Continued on next page*)

Continued

REAGENT or RESOURCE	SOURCE	IDENTIFIER
Chemicals, peptides, and recombinant proteins		
Lymphoprep™	STEMCELL Technologies	Cat#07801
Cisplatin	Sigma-Aldrich	Cat#P4394
Paraformaldehyde	Electron Microscopy Sciences	Cat#15710
Metal Contaminant-Free PBS	Rockland	Cat#MB-008
Brefeldin A Solution	Thermofisher	Cat#00-4506-51 s
PepMix SARS-CoV-2 Peptide (Spike Glycoprotein)	JPT Peptide Technologies	Cat#PM-WCPV-S
PMA	Sigma-Aldrich	Cat#1585
Ionomycin calcium salt	Sigma-Aldrich	Cat#I0634
Normal Mouse Serum	ThermoFisher	Cat#10410
Normal Rat Serum	ThermoFisher	Cat#10710C
Human Serum From Male AB Plasma	Sigma-Aldrich	Cat#H4511
Intracellular Fixation & Permeabilization Buffer	ThermoFisher	Cat#88-8823-88
Permeabilization Buffer	ThermoFisher	Cat#00-8333-56
Iridium Interchelator Solution	Fluidigm	Cat#201192B
MaxPar® cell staining buffer	Fluidigm	Cat#201068
Cell acquisition solution	Fluidigm	Cat#201240
EQ Four Element Calibration Beads	Fluidigm	Cat#201078
Critical commercial assays		
MaxPar® X8 Antibody Labeling Kit	Fluidigm	Cat#201169B
Cell-ID™ 20-Plex Pd Barcoding Kit	Fluidigm	Cat#201060
Deposited data		
Raw CyTOF datasets	This paper	http://datadryad.org/stash/dataset/doi:10.7272/Q67H1GTB
Software and algorithms		
FlowJo	BD Biosciences	https://www.flowjo.com/
Cytobank	Cytobank	https://www.cytobank.org/

RESOURCE AVAILABILITY

Lead contact

Requests for resources and reagents and for further information should be directed to and will be fulfilled by the Lead Contact, Nadia Roan (nadia.roan@gladstone.ucsf.edu).

Materials availability

This study did not generate new unique reagents.

Data and code availability

- The raw CyTOF datasets generated from this study are available for download through the public repository Dryad via the following link: http://datadryad.org/stash/dataset/doi:10.7272/Q67H1GTB
- This paper does not report original code.
- Any additional information required to reanalyze the data reported in this paper is available from the lead contact upon request.

EXPERIMENTAL MODEL AND SUBJECT DETAILS

Blood was drawn from 34 SARS-CoV-2-infected and 11 uninfected individuals. Infection status was established by RT-PCR. Of the infected individuals, 19 experienced a severe course of disease as defined by being in the ICU, and 6 of these individuals died from COVID-19 (designated "non-survivor" in this study). Moderate cases were defined as non-ICU hospitalizations for COVID-19. Eight

of the individuals that experienced severe disease were sampled longitudinally at up to 4 time points. All specimens from hospitalized patients were from a time point when the patients were still hospitalized, and this ranged from 0-76 days after initial positive SARS-CoV-2 test. Mild cases consisted of those never hospitalized for COVID-19, and were analyzed 20-154 after initial positive SARS-CoV-2 test. While specimens from mild, moderate, and severe cases may have been collected at similar times after infection, the specimens from the moderate and severe cases were from hospitalized individuals, and are therefore considered acute specimens. By contrast, specimens from the mild cases were from outpatient individuals that were no longer symptomatic at the time of sampling and therefore can be considered convalescent specimens. Additional clinical features, including patient gender, age, race, and whether patients were given convalescent plasma, dexamethasone, or remdesivir for COVID-19 (note patient COV06 was enrolled in a placebo-controlled remdesivir trial), are indicated in the table below. Consistent with male sex, advanced age, and non-white race being risk factors for severe disease, mild cases were predominantly female (81%, versus 48% for hospitalized patients), younger (median age 41, versus 64 for hospitalized patients), and all of white ethnicity (versus 72% LatinX for hospitalized patients). The demographics of severe fatal versus non-fatal cases of COVID-19 were more closely matched. In our cohort, fatal cases were more frequently female (67%, versus 54% for non-fatal), older (median age 73, versus 64 for non-fatal), and LatinX (100%, versus 61.5% for non-fatal). Hospitalized patients were all from the Zuckerberg San Francisco General Hospital (ZSFG), while out-patients were recruited from the COVID-19 Host Immune Pathogenesis (CHIRP) study. Importantly, all specimens were analyzed fresh, on the day of the blood draw, to avoid potential confounders associated with cell cryopreservation. This study was approved by the University of California, San Francisco (IRB # 20-30588).

Table: COVID-19 Patient Characteristics

Patient ID	Gender	Age	Race	Severity	Convalescent Plasma	Dexamethasone	Remdesivir	Days from discharge or death	Days between 1st PCR test and analysis
COV26	Female	84	LatinX	Moderate	No	No	Yes	8	2
COV21	Female	45	LatinX	Moderate	No	No	Yes	1	6
COV16	Female	47	AA	Moderate	No	No	No	0	13
COV25	Male	53	LatinX	Moderate	No	No	No	20	1
COV06	Male	54	LatinX	Moderate	No	No	Yes	3	8
COV07	Male	61	Asian	Moderate	Yes	No	Yes	5	11
COV14	Male	48	Asian	Severe	No	Yes	Yes	8	15
COV05	Male	72	LatinX	Severe	Yes	No	No	34	28
COV13	Female	64	AA	Severe	No	No	Yes	11	10
COV42	Female	74	LatinX	Severe	No	Yes	Yes	8	8
COV47	Female	66	AA	Severe	No	Yes	Yes	25	0
COV61	Female	69	Asian	Severe	No	No	Yes	5	14
COV04	Male	76	Asian	Severe	No	No	No	4	54
COV80	Female	59	LatinX	Severe	No	Yes	Yes	1	26
COV08	Male	47	LatinX	Severe	No	No	No	56	1
COV12								30	27
COV17								16	41
COV03	Male	61	LatinX	Severe	No	No	Yes	35	57
COV11								16	76
COV19	Male	65	LatinX	Severe	Yes	No	Yes	NA	32
COV37								NA	42
COV20	Female	59	LatinX	Severe	Yes	Yes	Yes	56	10
COV38								46	20
COV53b								32	34
COV69								28	38
COV31	Male	60	LatinX	Severe	Yes	No	No	45	7
COV46								43	9
COV74								25	27
COV86								17	35
COV01	Female	30	LatinX	Severe/ Death	No	No	Yes	35	14

(*Continued on next page*)

Continued

Patient ID	Gender	Age	Race	Severity	Convalescent Plasma	Dexamethasone	Remdesivir	Days from discharge or death	Days between 1st PCR test and analysis
COV18	Female	75	LatinX	Severe/ Death	Yes	Yes	Yes	12	10
COV15	Female	82	LatinX	Severe/ Death	No	No	Yes	8	9
COV02 COV10	Female	82	LatinX	Severe/ Death	No	No	Yes	19 0	2 21
COV22 COV24 COV39	Male	65	LatinX	Severe/ Death	Yes	Yes	Yes	39 13 11	5 13 15
COV45 COV62	Male	71	LatinX	Severe/ Death	Yes	No	No	14 3	7 21
PID4123	Male	33	White	Mild	No	No	No	NA	25
PID4103	Female	41	White	Mild	No	No	No	NA	20
PID4100	Female	28	White	Mild	No	No	No	NA	36
PID4114	Female	45	White	Mild	No	No	No	NA	59
PID4104	Female	33	White	Mild	No	No	No	NA	60
PID4122	Female	33	White	Mild	No	No	No	NA	26
PID4106	Female	67	White	Mild	No	No	No	NA	46
PID4112	Female	59	White	Mild	No	No	No	NA	154
PID4102	Male	46	White	Mild	No	No	No	NA	47

METHOD DETAILS

Preparation of specimens for CyTOF

On the day of each blood draw, PBMCs were isolated from blood using Lymphoprep™ (StemCell Technologies). Six million cells were then immediately treated with cisplatin (Sigma-Aldrich) as a live/dead marker and fixed with paraformaldehyde (PFA) as previously described (Ma et al., 2020; Neidleman et al., 2020a), unless there were insufficient cell numbers in which case fewer cells were treated in this manner. Fixation was carried out by resuspending cells in 2 mL PBS (Rockland) with 2 mM EDTA (Corning), and then adding 2 mL of PBS containing 2 mM EDTA and 25 μM cisplatin (Sigma-Aldrich). After 1 min of incubation, cisplatin staining was quenched with 10 mL of CyFACS (metal contaminant-free PBS (Rockland) supplemented with 0.1% bovine serum albumin (BSA) and 0.1% sodium azide (Sigma-Aldrich)). The cells were then centrifuged, resuspended in 2% PFA in CyFACS, and incubated for 10 minutes at room temperature. After two more washes with CyFACS, cells were resuspended in CyFACS containing 10% DMSO and stored at −80°C until analysis by CyTOF. These cells constituted the "baseline" specimens, and enabled the characterization of the phenotypes of total, unstimulated T cells from COVID-19 patients.

The remaining cells were stimulated for 6 hours with the co-stimulatory agents 0.5 μg/ml anti-CD49d clone L25 and 0.5 μg/ml anti-CD28 clone L293 (both from BD Biosciences) and 0.5 μM of overlapping 15-mer SARS-CoV-2 spike peptides PepMix SARS-CoV-2 Peptide (Spike Glycoprotein) (JPT Peptide Technologies) in RP10 media (RPMI 1640 medium (Corning) supplemented with 10% fetal bovine serum (FBS, VWR), 1% penicillin (GIBCO), and 1% streptomycin (GIBCO)). These peptides cover both the S1 and S2 domains of the spike protein. To test the functionality of the IL6 antibody, PBMCs were stimulated instead with 200 ng/ml lipopolysaccharide LPS (Sigma-Aldrich). A final concentration of 3 μg/ml Brefeldin A Solution (eBioscience) was also included to enable detection of intracellular cytokines. For samples that had sufficient cell yield, a positive control of stimulation with 16 nM PMA (Sigma-Aldrich) and 1 μM ionomycin (Sigma-Aldrich) was additionally included. Treated cells were then cisplatin-treated and PFA-fixed as described above.

CyTOF staining and data acquisition

CyTOF staining was conducted using recently described methods (Cavrois et al., 2017; Ma et al., 2020; Neidleman et al., 2020a, 2020b), using a CyTOF panel designed to include multiple markers of T cell differentiation state, activation status, exhaustion, proliferative potential, and homing properties (see table below). Antibodies were either purchased from the indicated vendor or prepared in-house using commercially available MaxPAR conjugation kits per manufacturer's instructions (Fluidigm). Cisplatin-treated cells were thawed and washed with CyFACS in Nunc 96 DeepWell™ polystyrene plates (Thermo Fisher) at a concentration of 6×10^6 cells / 800 μL in each well. Cells were then blocked with mouse (Thermo Fisher), rat (Thermo Fisher), and human AB (Sigma-Aldrich) sera

for 15 minutes at 4°C. Samples were then washed twice in CyFACS and stained at 4°C for 45 minutes with surface CyTOF antibodies (see table below) in a final volume of 100 μl. The samples were then washed three times with CyFACS, and fixed overnight at 4°C in 100 μL of 2% PFA in PBS. Samples were then washed twice with Intracellular Fixation & Permeabilization Buffer (eBioscience) and incubated for 45 minutes at 4°C. After two additional washes with Permeabilization Buffer (eBioscience), samples were blocked for 15 minutes at 4°C in 100 μL of mouse and rat sera diluted in Permeabilization Buffer. After another round of washing with Permeabilization Buffer, samples were stained at 4°C for 45 minutes with intracellular CyTOF antibodies (indicated by asterisk in table below) in a final volume of 100 μl. The intracellular antibodies included the transcription factors Tbet, RORγt, and NFAT, as well as the cytokines IFNγ, IL4, IL5, IL6, and IL17. Of note, GATA3 was not included in the panel as we were unable to validate staining of this Th2 transcription factor. The cells were then washed with CyFACS, and stained for 20 minutes at room temperature with 250 nM of Cell-ID™ Intercalator-IR (Fluidigm). Immediately prior to sample acquisition, cells were washed twice with CyFACS buffer, once with Max-Par® cell staining buffer (Fluidigm), and once with Cell acquisition solution (CAS, Fluidigm), and then resuspended in EQ Four Element Calibration Beads (Fluidigm) diluted in CAS. Samples were acquired on a Helios-upgraded CyTOF2 instrument (Fluidigm) at the UCSF Parnassus flow core facility.

Table: List of CyTOF antibodies used in study (asterisks correspond to antigens analyzed intracellularly).

Antigen Target	Clone	Elemental Isotope	Vendor
HLADR	TÜ36	Qdot (112Cd)	Thermofisher
RORγt*	AFKJS-9	115 In	In-house
CD49d (α4)	9F10	141Pr	Fluidigm
CTLA4*	14D3	142Nd	In-house
NFAT*	D43B1	143Nd	Fluidigm
CCR5	NP6G4	144Nd	Fluidigm
IL5*	TRFK5	145Nd	In-house
CD95	BX2	146Nd	In-house
CD7	CD76B7	147Sm	Fluidigm
ICOS	C398.4A	148Nd	Fluidigm
Tbet*	4B10	149Sm	In-house
IL4*	MP4-25D2	150Nd	In-house
CD2	TS1/8	151Eu	Fluidigm
IL17*	BL168	152Sm	In-house
CD62L	DREG56	153Eu	Fluidigm
TIGIT	MBSA43	154Sm	Fluidigm
CCR6	11A9	155Gd	In-house
IL6*	MQ2-13A5	156 Gd	In-house
CD8	RPA-T8	157Gd	In-house
CD19	HIB19	157Gd	In-house
CD14	M5E2	157Gd	In-house
OX40	ACT35	158Gd	Fluidigm
CCR7	G043H7	159Tb	Fluidigm
CD28	CD28.2	160Gd	Fluidigm
CD45RO	UCHL1	161Dy	In-house
CD69	FN50	162Dy	Fluidigm
CRTH2	BM16	163Dy	Fluidigm
PD-1	EH12.1	164Dy	In-house
CD127	A019D5	165Ho	Fluidigm
CXCR5	RF8B2	166Er	In-house
CD27	L128	167Er	Fluidigm
IFNγ*	B27	168Er	Fluidigm
CD45RA	HI100	169Tm	Fluidigm
CD3	UCHT1	170Er	Fluidigm
CD57	HNK-1	171Yb	In-house

(*Continued on next page*)

Continued

Antigen Target	Clone	Elemental Isotope	Vendor
CD38	HIT2	172Yb	Fluidigm
α4β7	Act1	173Yb	In-house
CD4	SK3	174Yb	Fluidigm
CXCR4	12G5	175Lu	Fluidigm
CD25	M-A251	176Yb	In-house
CD161	NKR-P1A	209 Bi	In-house

QUANTIFICATION AND STATISTICAL ANALYSIS

CyTOF data analysis

CyTOF datasets were exported as flow cytometry standard (FCS) files, and de-barcoded according to manufacturer's instructions (Fluidigm). FlowJo software (BD Biosciences) was used to identify $CD4^+$ T cells (live, singlet $CD3^+CD19^-CD4^+CD8^-$) and $CD8^+$ T cells (live, singlet $CD3^+CD19^-CD4^-CD8^+$) among the baseline and stimulated samples. Peptide-stimulated samples were further separated into bystander ($IFN\gamma^-$) and SARS-CoV-2-specific ($IFN\gamma^+$) T cells. $IFN\gamma^+$ cells were detected in the stimulated samples from all three patient groups and amounted to a total of 3,735 cells. For subset and high-dimensional analyses of SARS-CoV-2-specific T cells, we excluded patients with fewer than three SARS-CoV-2-specific T cells to limit skewing of data. All subset percentages were reported relative to number of live, singlet PBMCs, or the indicated T cell subset. t-SNE analyses were performed using the Cytobank software with default settings. All phenotyping cellular markers not used in the upstream gating strategy were included in generating the t-SNE plots. Non-cellular markers (e.g., live/dead stain) and cytokines were excluded for the generation of t-SNE plots. Dot plots were generated using both Cytobank and FlowJo. Clustering was conducted using the unsupervised clustering algorithm FlowSOM (Van Gassen et al., 2015) within Cytobank, using default settings (Clustering method: Hierarchical consensus; Iterations: 10; Seed: Automatic). The same parameters used in t-SNE plot generation were used as FlowSOM clustering parameters. The statistical tests used in comparison of groups are indicated within the figure legends.

Antibody Measurement

IgM and IgG antibodies against SARS-CoV-2 spike receptor binding domain (RBD) and nucleocapsid protein (NP) were measured in samples from patients that did not receive convalescent plasma, using the Pylon 3D automated immunoassay system (ET Healthcare) as described (Lynch et al., 2021). Briefly, quartz glass probes precoated with either affinity-purified goat anti-human IgM (to capture IgM) or Protein G (to capture IgG) were dipped into 15 μL of diluted patient plasma. After washing, the probe was dipped into the assay reagent containing both biotinylated recombinant RBD and NP. After additional washes, the probe was incubated with a Cy5-conjugated streptavidin polysaccharide conjugate reagent. The background-corrected signal was reported as relative fluorescent units (RFU), reflecting the relative levels of specific antibodies in each specimen.

Analysis of public scRNaseq datasets of COVID-19 bronchoalveolar lavage specimens

FASTQ files generated from BAL samples of two moderate (GSM4339769, GSM4339770) and six severe/critical patients were downloaded from the Gene Expression Omnibus (GEO) database under accession code GSE145926 (https://www.ncbi.nlm.nih.gov/geo/query/acc.cgi?acc=GSE145926) (Liao et al., 2020). These scRNaseq datasets were generated using the Chromium Single Cell 5′ library preparation kit (10X Genomics). Cell Ranger software version 3.1.0 (10x Genomics) was used to generate the filtered cell-barcode matrices. A standard Seurat v.3 workflow (Stuart et al., 2019) was used to generate cell clusters after filtering out dead cells (those containing more than 10% of mitochondrial gene counts). T and epithelial cell clusters were then extracted from each sample, by identification of clusters expressing the CD3 and EPCAM genes, respectively. The filtered gene-barcode matrices for the extracted cells were normalized using 'LogNormalize' with default parameters. The top 2,000 variable genes were then identified using the 'vst' method by the 'FindVariableFeatures' function. To integrate the 8 BAL samples and remove potential batch effects, we used the standard integration Seurat v.3 workflow. The first 30 dimensions from canonical correlation analysis (CCA) were used as the input parameter for the 'FindTransferAnchors' function. Principal component analysis (PCA) was performed using the top 2,000 variable genes of the integrated matrix, followed by implementation of the graph-based clustering algorithm on the PCA-reduced data. Finally, UMAP visualizations were generated using the top 30 PCA. The UMAP resolution was set to 0.8. To detect SARS-CoV-2 transcripts, a customized reference genome/transcriptome was built by integrating the both human GRCh38 and SARS-CoV-2 genomes (severe acute respiratory syndrome coronavirus 2 isolate Wuhan-Hu-1, complete genome, GenBank MN908947.3 (https://www.ncbi.nlm.nih.gov/nuccore/MN908947.3/)). FASTQ alignment was performed using the splice-aware aligner STAR (Dobin et al., 2013).